LEVEL II (5)

AFGL-TR-81-0238

CHATANIKA RADAR MEASUREMENTS DURING THE AURORAL E PROGRAM

Robert M. Robinson
Richard R. Vondrak

SRI International
333 Ravenswood Avenue
Menlo Park, California 94025

Scientific Report No. 1

June 1981

Approved for public release; distribution unlimited.

AIR FORCE GEOPHYSICS LABORATORY
AIR FORCE SYSTEMS COMMAND
UNITED STATES AIR FORCE
HANSCOM AFB, MASSACHUSETTS 01731

UNCLASSIFIED

SECURITY CLASSIFICATION OF THIS PAGE (When Data Entered)

REPORT DOCUMENTATION PAGE	READ INSTRUCTIONS BEFORE COMPLETING FORM
1. REPORT NUMBER: AFGL-TR-81-0238	2. GOVT ACCESSION NO.: AD-A107 217
	3. RECIPIENT'S CATALOG NUMBER
4. TITLE (and Subtitle): CHATANIKA RADAR MEASUREMENTS DURING THE AURORAL E PROGRAM	5. TYPE OF REPORT & PERIOD COVERED: Scientific Report No. 1
	6. PERFORMING ORG. REPORT NUMBER: SRI Project 2734
7. AUTHOR(s): Robert M. Robinson and Richard R. Vondrak	8. CONTRACT OR GRANT NUMBER(s): F19628-81-K-0037
9. PERFORMING ORGANIZATION NAME AND ADDRESS: SRI International, 333 Ravenswood Ave., Menlo Park, CA 94025	10. PROGRAM ELEMENT, PROJECT, TASK AREA & WORK UNIT NUMBERS: 62101F, 4643[illegible]BC, 17 96
11. CONTROLLING OFFICE NAME AND ADDRESS: Air Force Geophysics Laboratory, Hanscom AFB, MA 01731, Monitor/B.S. Dandekar/(AFGL/PHY)	12. REPORT DATE: June 1981
	13. NUMBER OF PAGES: 48
14. MONITORING AGENCY NAME & ADDRESS (if different from Controlling Office)	15. SECURITY CLASS (of this report): UNCLASSIFIED
	15a. DECLASSIFICATION/DOWNGRADING SCHEDULE

16. DISTRIBUTION STATEMENT (of this Report)

Approved for public release; distribution unlimited.

17. DISTRIBUTION STATEMENT (of the abstract entered in Block 20, if different from Report)

18. SUPPLEMENTARY NOTES

19. KEY WORDS (Continue on reverse side if necessary and identify by block number)

Diffuse aurora
Continuous aurora
Auroral ionization
Particle precipitation
Electric fields
Chatanika radar

20. ABSTRACT (Continue on reverse side if necessary and identify by block number)

Chatanika radar electron-density and electric-field measurements were made during the Auroral E rocket program ~~of February and March 1981~~. Four instrumented sounding rockets were launched ~~on the evening of 7 March~~ into the diffuse aurora from Poker Flat Research Range near Fairbanks, Alaska. The radar provided ionospheric data during eight consecutive nights preceding the launch. The radar data from the night of the launch were analyzed to determine the extent and duration of the auroral E layer. The

DD FORM 1 JAN 73 1473 EDITION OF 1 NOV 65 IS OBSOLETE

UNCLASSIFIED

SECURITY CLASSIFICATION OF THIS PAGE (When Data Entered)

410 281

electron density data indicated that the southward advance of the diffuse aurora was consistent with the average shape of the statistical auroral oval. During the rocket launches the E layer was uniform with a maximum density of about 2 to 3 x 10^5 el/cm^3 at an altitude of 125 km. The energy flux of precipitating electrons was 1.5 to 2.0 ergs/cm^2-sec. The mean energy of the electrons was inferred to be about 2 keV. Electric fields were northward with a magnitude of 30 mV/m. No auroral arcs were present within the range of the rocket trajectories.

CONTENTS

ILLUSTRATIONS

TABLES

I INTRODUCTION

As part of the Auroral E Program to study the continuous or diffuse aurora, the Air Force Geophysics Laboratory (AFGL) launched four sounding rockets on the evening of 7 March 1981. The payloads were launched from the Poker Flat Research Range, Alaska and carried instrumentation to measure particle fluxes, optical emissions, ionization, and electric fields, as well as properties of the neutral atmosphere. Coordinated measurements were made by the Chatanika radar, the AFGL Airborne Ionospheric Observatory, and several ground-based optical stations. The primary objective of this experiment was to assess the validity of theoretical models used to deduce ionization profiles from satellite and ground-based data. The launch criteria for the rocket experiments were based on the requirement that the ionosphere be spatially uniform and that steady conditions exist. The Chatanika radar was operated for nine consecutive nights during the program. The purpose of the radar measurements was twofold: first, the real-time data were used to determine if the launch criteria were satisfied; and second, postflight analysis of the radar data provides ionospheric information necessary for testing the accuracy of the theoretical models.

In this report, we present and interpret the Chatanika radar data that were obtained on the evening of 7 March 1981. The radar was operated in several different modes to provide diagnostic information before, during, and after the rocket launches. Here, we summarize those observations and briefly describe the extent to which the launch criteria were satisfied.

II CHATANIKA RADAR OPERATING MODES

The Chatanika radar is an incoherent-scatter facility located 27 miles north of Fairbanks, Alaska. The radar antenna is a fully steerable dish with a diameter of 27 m. It transmits at a frequency of 1290 MHz at 4-MW peak power. The radar system has been described by Baron [1977]. The return signal is processed to yield electron density and line-of-sight ion-drift velocity as a function of range. By steering the antenna appropriately during data acquisition, the spatial distribution of electron density can be determined and the vector electric field can be computed. Details of the methods by which ionospheric parameters are obtained from electron density are given in de la Beaujardiere et al. [1980]. The operating modes used during the Auroral E Program are summarized below.

A. Meridian Scans

In the meridian scan mode, the antenna scans in elevation in the magnetic meridian plane. For the Auroral E Program, full scans extended from 15° north elevation to 35° south elevation as shown in Figure 1. The scan lasted about 12 min. The scanning rate was reduced when the elevation angle was less than 55° to allow the use of longer integration times without sacrificing spatial resolution. Partial meridian scans during the Auroral E Program extended from 30° elevation to 77° south elevation (magnetic zenith). Partial scans took about four minutes to complete.

Meridian scan data are processed to yield altitude-latitude profiles of electron density and ion-drift velocity. Two pulses are transmitted: a 60-μs pulse followed by a 320-μs pulse. Electron density is determined from short- and long-pulse returns. The short pulses provide density measurements of 9 km resolution, while the long pulses provide a resolution of 48 km. Drift velocity is computed from spectral analysis of

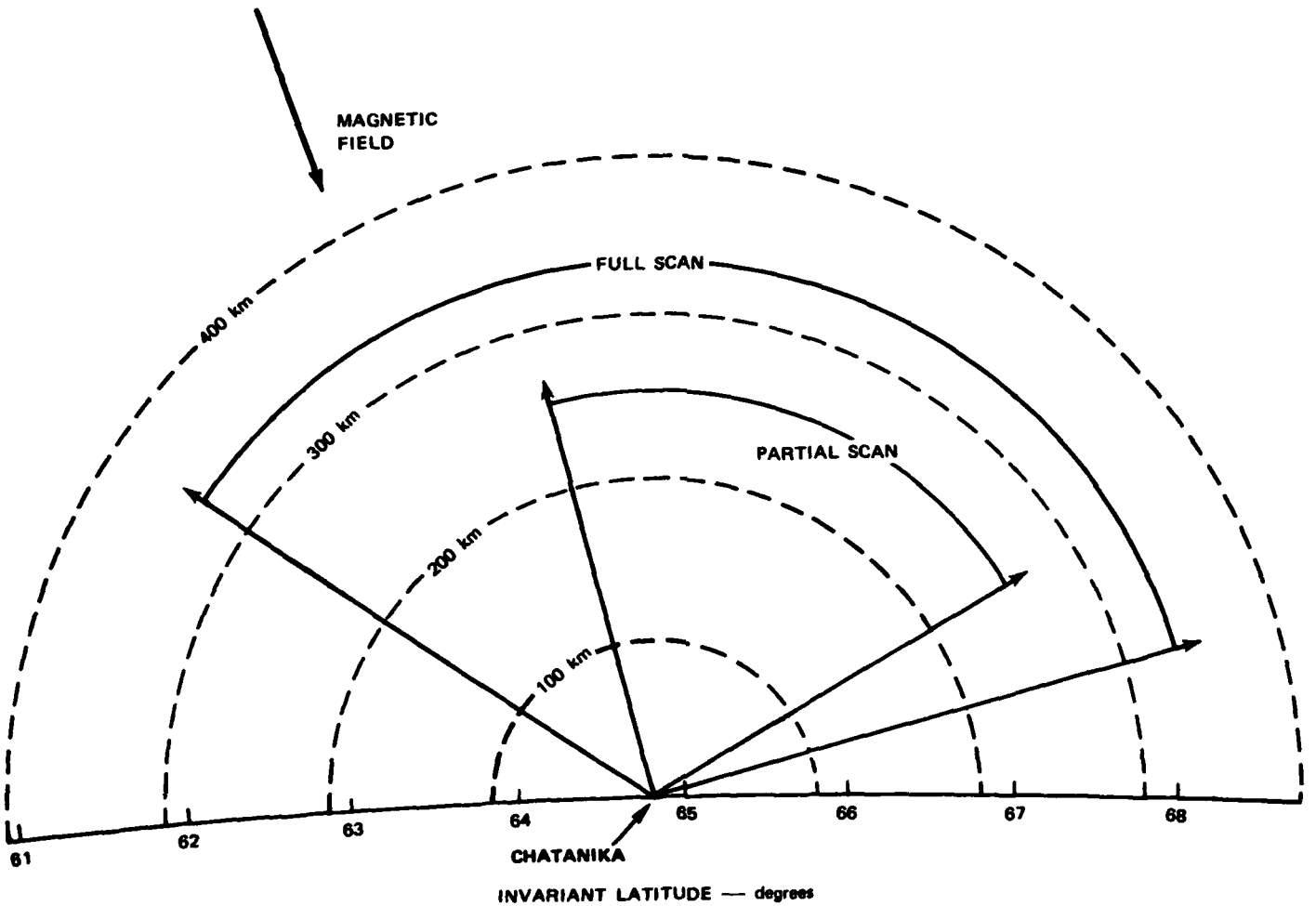

FIGURE 1 EXTENT OF MERIDIAN SCANS USED IN AURORAL-E ROCKET SUPPORT

long-pulse returns. In the meridian scan mode, only the line-of-sight velocity component within the meridian plane is measured. In most cases, the component of velocity along the magnetic field is small so that the perpendicular ion drift within the meridian plane can be determined from a single measurement. In the F region, this gives the east-west electric field. By combining the east-west electric field with the meridional ion drift in the E region, the north-south electric field can be computed [de la Beaujardiere et al., 1981].

B. Azimuth Scans

In this mode, the antenna scans in azimuth at a constant elevation angle. For the auroral-E rocket support, the elevation angle was 40°. The E- and F-region intercepts of the antenna beam are shown in Figure 2. The scan limits were 45° north and south from magnetic east. The scan lasted 5 min. The transmitted-pulse pattern was the same as that used during the meridian scans.

In the azimuth-scan mode, ion-drift velocity measurements at F-region altitudes are used to compute a latitudinal profile of the electric field. At azimuths close to magnetic east or west the north-south electric field is determined from the line-of-sight drift velocity. The full vector electric field can be computed by combining these measurements with east-west electric field measurements obtained during a previous or subsequent elevation scan. The earth's rotation during the two scans insures that the two components of the electric field are measured at approximately the same magnetic local time. This technique for measuring electric fields complements the elevation-scan technique because it provides vector measurements within the Chatanika L shell. In the elevation-scan mode, this is not possible because the radar line of sight is parallel to the magnetic field lines and horizontal drifts cannot be measured. The azimuth scan technique also allows accurate measurement of drifts as long as the F-region electron density is $> 10^5$ el/cm^3. In contrast, the elevation scan technique requires a high E region density.

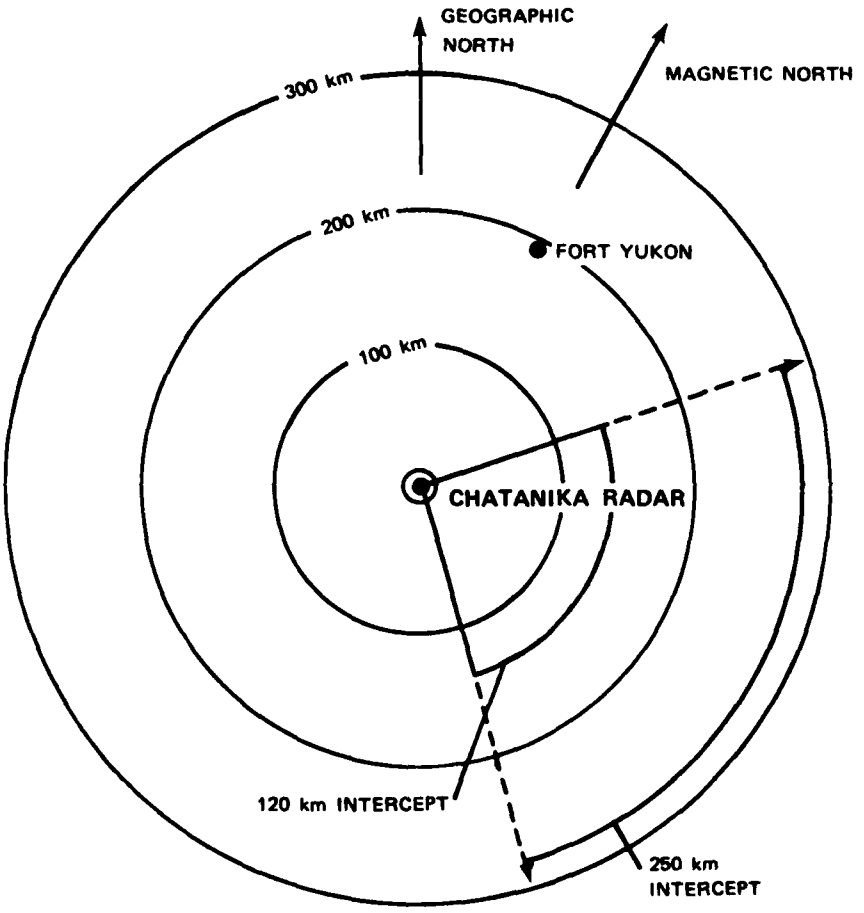

FIGURE 2 E- AND F-REGION INTERCEPTS OF ANTENNA BEAM DURING AZIMUTH SCANS USED IN AURORAL-E ROCKET SUPPORT

C. Fixed Position

In this mode the antenna position is fixed for periods of two to five min. The long integration times yield very accurate measurements of the line-of-sight ion-drift velocity and the spectral shape. From the spectral shape other ionospheric parameters, such as the ion and electron temperatures, can be obtained. When three noncolinear fixed-position measurements are combined, the full vector-drift velocity can be determined. From this, the vector electric field is computed along with the E-region neutral wind. This technique for measuring electric fields differs from those described above in that it yields one spatially averaged measurement. Spatial inhomogeneities in the ionospheric drift over distances less than the beam separation can distort the measurements. This technique also requires temporal stability over the period during which the three measurements are made.

For the Auroral E Program, the three positions used were 70° north elevation in the magnetic meridian, 70° east elevation in the magnetic L shell and 76° south elevation in the magnetic meridian (along the magnetic field). The E- and F-region intercepts of the three beam positions are shown in Figure 3. The dwell time in each position was four min. The transmitted pulse pattern was 60 μs, 320 μs, 160 μs, and 160 μs. The latter two pulses are used to obtain high-resolution E-region neutral-wind measurements [Rino et al., 1974]. With sufficiently long integration times, electron and ion temperatures can also be computed in the altitude range 80 to 180 km.

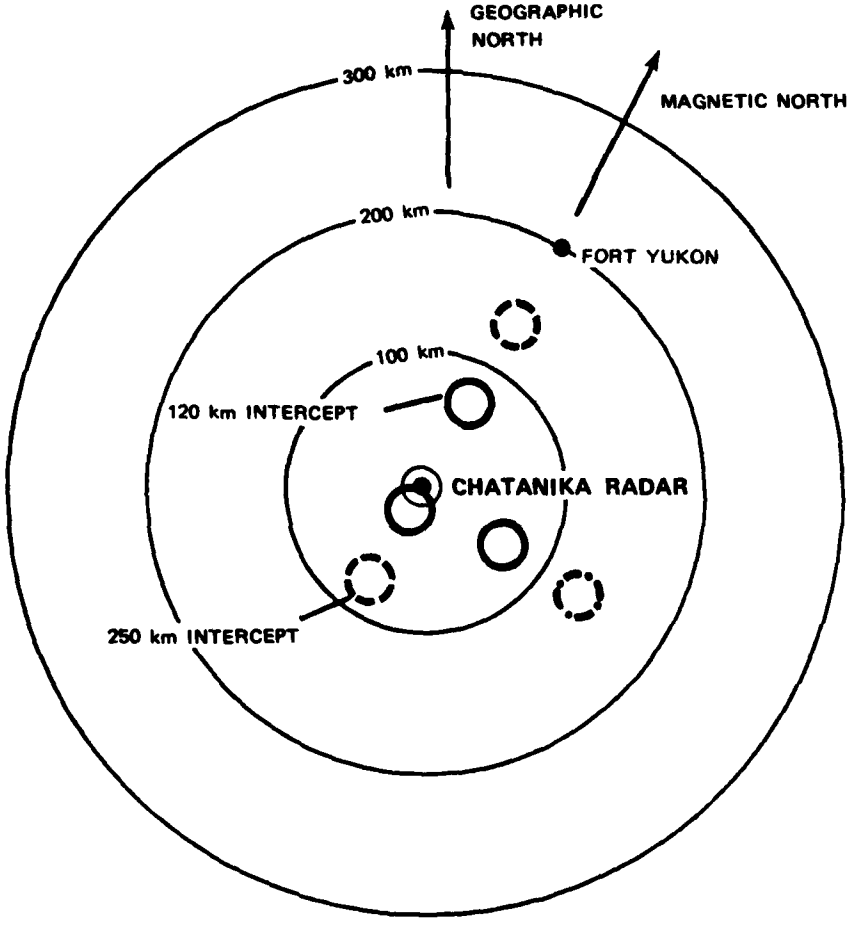

FIGURE 3 E- AND F-REGION INTERCEPTS OF ANTENNA BEAM FOR THREE FIXED POSITIONS USED IN AURORAL-E EXPERIMENT

III RADAR OPERATIONS DURING THE AURORAL E PROGRAM

The Chatanika radar was operated for nine consecutive nights during the Auroral E Program. The hours of operation on each night are listed in Table 1. The radar was operated in a meridian scan mode alternated with azimuth scans. For most of this time period auroral activity was high, and the launch criterion of spatial uniformity was not met. The rocket launches were delayed for several nights because of cloudy weather.

Table 1

HOURS OF RADAR OPERATIONS AND AIRCRAFT FLIGHT TIMES DURING AURORAL-E PROGRAM

Date	Hours of Operation (UT)	AIO Aircraft Flight Times (UT)
27 February	0514 to 1045	
28 February	0551 to 1403	0759-1244
1 March	0602 to 1231	0820-1200
2 March	0541 to 1043	
3 March	0442 to 1000	
4 March	0003 to 2400	
5 March	0440 to 1224	
6 March	0451 to 1316	
7 March	0453 to 1300	0740-0947

During several nights early in the launch window, attempts were made to coordinate the rocket launches with an overpass by the P 78-1 satellite. P 78-1 satellite passes occurred each night at about 1000 UT and 1130 UT. These passes were fixed in local time such that the earlier pass occurred 400 km to the east of Chatanika and the later pass was 400 km to the west. The flight path of the AIO aircraft was chosen so

that ionospheric data linking the satellite trajectory and the launch meridian could be obtained. The hours during which the aircraft was in flight are shown in Table 1.

After several nights during which the launch criteria were not met, the requirement of coordinating with the satellite was relaxed and the launch windows were extended to earlier local times.

Chatanika operations on the evening of the rocket launches are summarized in Table 2. The last column in Table 2 indicates the launch times of each of the four rockets. When radar operations began at 0453 UT (1853 AST*) E-region densities were $< 2 \times 10^4$ el/cm. However, the F-region ionization was everywhere greater than several times 10^5. As the evening progressed, E-region densities above 2×10^4 appeared far to the north. This increase in ionization was also confirmed by enhanced optical emissions observed from Fort Yukon, Alaska. This gradual increase in ionization continued until the diffuse aurora in the north became visible to observers at Poker Flat. The diffuse aurora was bounded in the north by a rayed arc.

At 0740 UT, the AFGL aircraft was deployed. As the aircraft executed its flight pattern, the diffuse aurora continued to move southward, but remained fairly uniform. All discrete arcs were still well to the north of the rocket trajectories. This auroral pattern persisted throughout the four rocket launches. All four rockets were launched successfully; telemetry was good and preliminary indications were that all instruments functioned properly.

Launch and trajectory information for the four rockets is given in Table 3. The TMA was released at 0840 UT and tracked optically for about 30 min. At 1000 UT, the diffuse aurora moved to the south and bright auroral arcs and rays appeared overhead.

---

*Alaska Standard Time.

Table 2

RADAR OPERATIONS ON 7 MARCH 1981

Time (UT)	Operating Mode	Launch Times
0453 to 0736	Full meridian scans alternated with three-min fixed-position in the magnetic zenith.	
0737 to 0742	Five-min azimuth scan to the east	
0742 to 0755	One full meridian scan	
0756 to 0801	Five-min azimuth scan to the east	
0803 to 0834	Seven partial meridian scans from magnetic zenith to 30° N elevation	0809:00 (A13.030) 0809:58 (A13.020) 0826:00 (A13.031)
0834 to 0849	Switch to multiple-pulse mode	0838:00 (A10.903)
0849 to 0909	Five fixed-position dwells--four-min each. One in magnetic zenith, two at 70° elevation in magnetic meridian and two at 70° elevation in the L shell	
0912 to 0924	One full meridian scan	
0931 to 0939	Two four-min partial meridian scans to the north	
>0939	Meridian scans with fixed position	

Table 3

AURORAL-E ROCKET PAYLOAD AND LAUNCH INFORMATION

Payload	Instrumentation	Flight Time (UT)	Apogee Altitude (km)
(1) A13.030	Electron Proton Spectrometer Six-Channel Photometer Five-Channel VUV Photometer	0809:00 to 0817:52	156.40
(2) A13.020	Mass Spectrometer NRL Pulsed Plasma Probes Electron Density Spectrometer	0809:58 to 0818:27	202.71
(3) A13.031	Electron Proton Spectrometer 2 Spectrometers 1 Photometer	0826:00 to 0834:41	169.66
(4) A10.903	Falling Sphere E-field Booms TMA Release	0838:00 to 0845:16	186.24

IV RADAR MEASUREMENTS ON 7 MARCH 1981

A. Radar Measurements From 0453 to 0803 UT

During this time period the radar completed ten full elevation scans in the magnetic meridian. Electron density contour plots from three of these scans are shown in Figures 4 through 6. In these plots electron density is plotted as a function of invariant latitude and altitude along a field line (i.e. magnetic field lines are vertical). Electron-density contours are drawn at intervals of 2×10^4 el/cm^3. These contour plots are generated by combining data from field-aligned electron-density profiles at horizontal intervals of 5 to 30 km. Each individual profile is constructed by merging short-pulse density data in the altitude range from 60 to 160 km with long-pulse data above 160 km. The data have been smoothed in altitude and partially corrected for the effects of temperature. The latter correction must be applied because the power returned is a function of the electron-to-ion temperature ratio and the Debye length. The Debye length correction is made by assuming a model temperature profile from Jacchia [1975]. The ion-electron temperature ratio was assumed to be unity, because temperature data is not presently available.

A striking feature in Figures 4 through 6 is the very intense F region with densities as high as 1×10^6 el/cm^3. Because the F-region electron density increases to the south, this ionization is probably solar produced. The solar zenith angle at Chatanika at 0500 UT was 101° so that the ionosphere above 100 km was sunlit. In contrast, the E-region density increases to the north, suggesting production by auroral zone precipitation. This ionization pattern is typical of that usually observed at the equatorward edge of the diffuse aurora. For the purposes of this report, we define the diffuse aurora as regions where the E-region ionization is above 1×10^5 el/cm^3. Arcs are identified as regions where the E-region ionization exceeds 3×10^5 el/cm^3 and contains

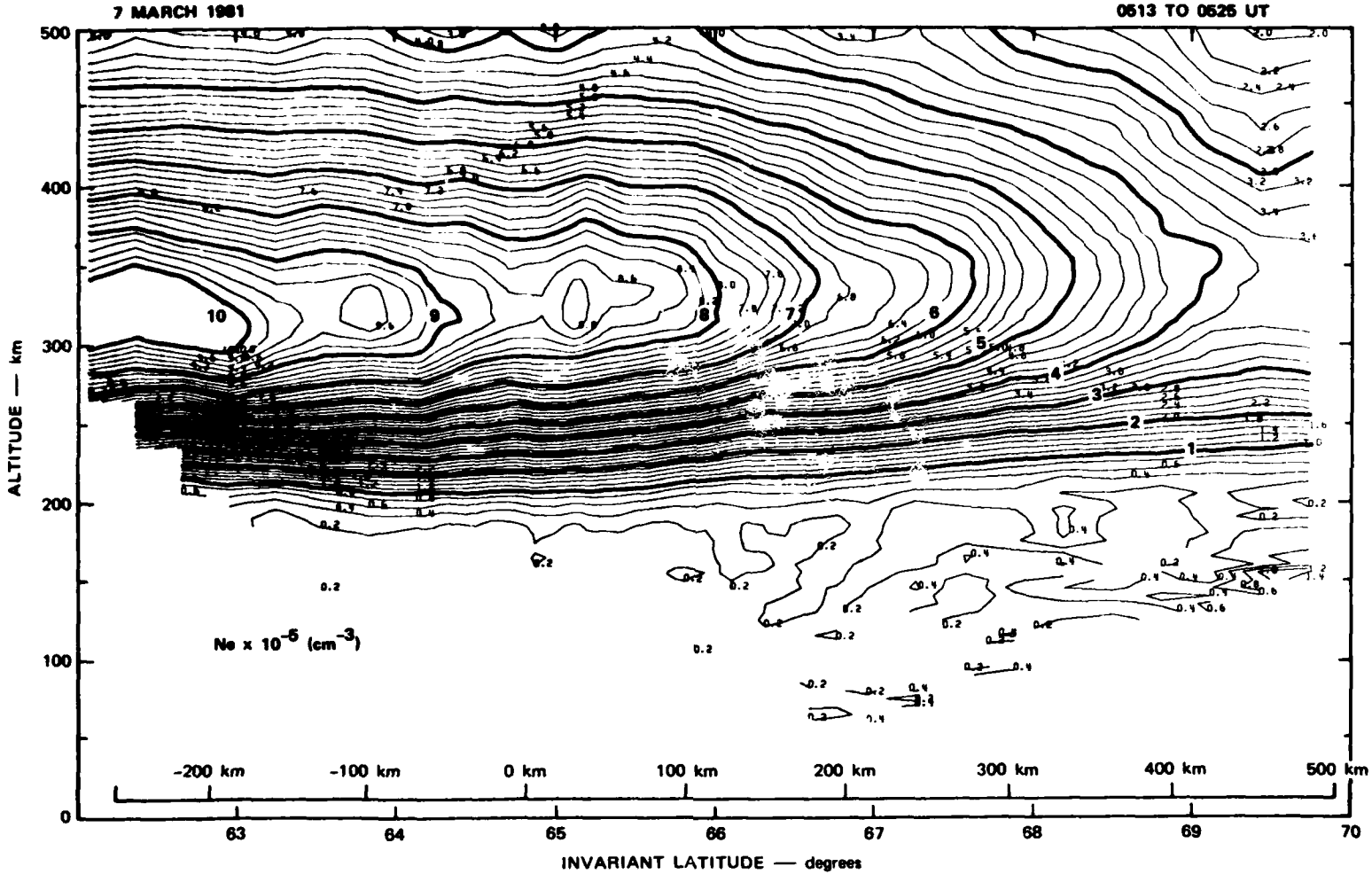

FIGURE 4 ELECTRON-DENSITY CONTOUR PLOT CONSTRUCTED FROM FULL MERIDIAN SCAN BEGINNING AT 0512:48 UT

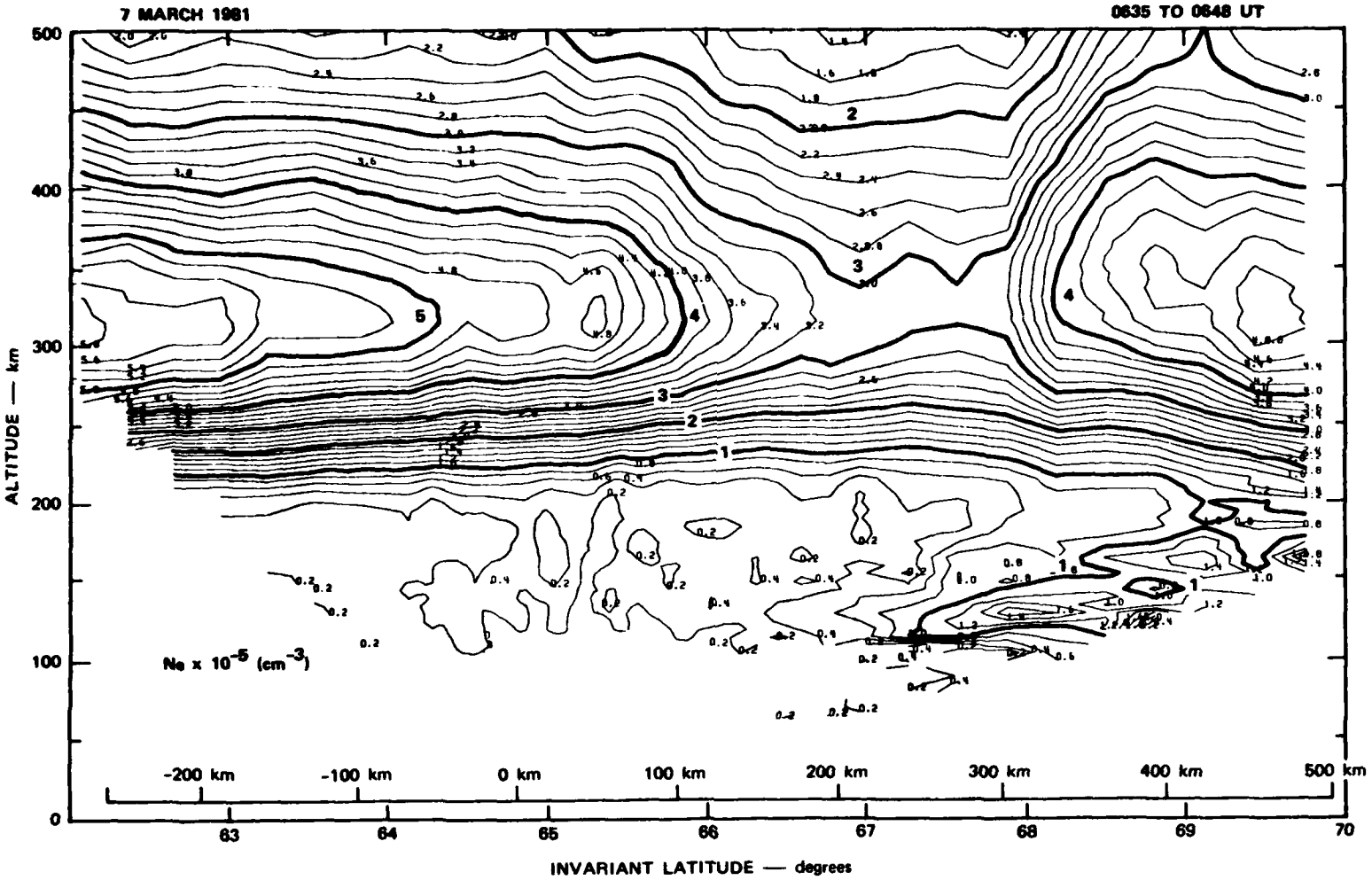

FIGURE 5 ELECTRON-DENSITY CONTOUR PLOT: 0635 TO 0648 UT

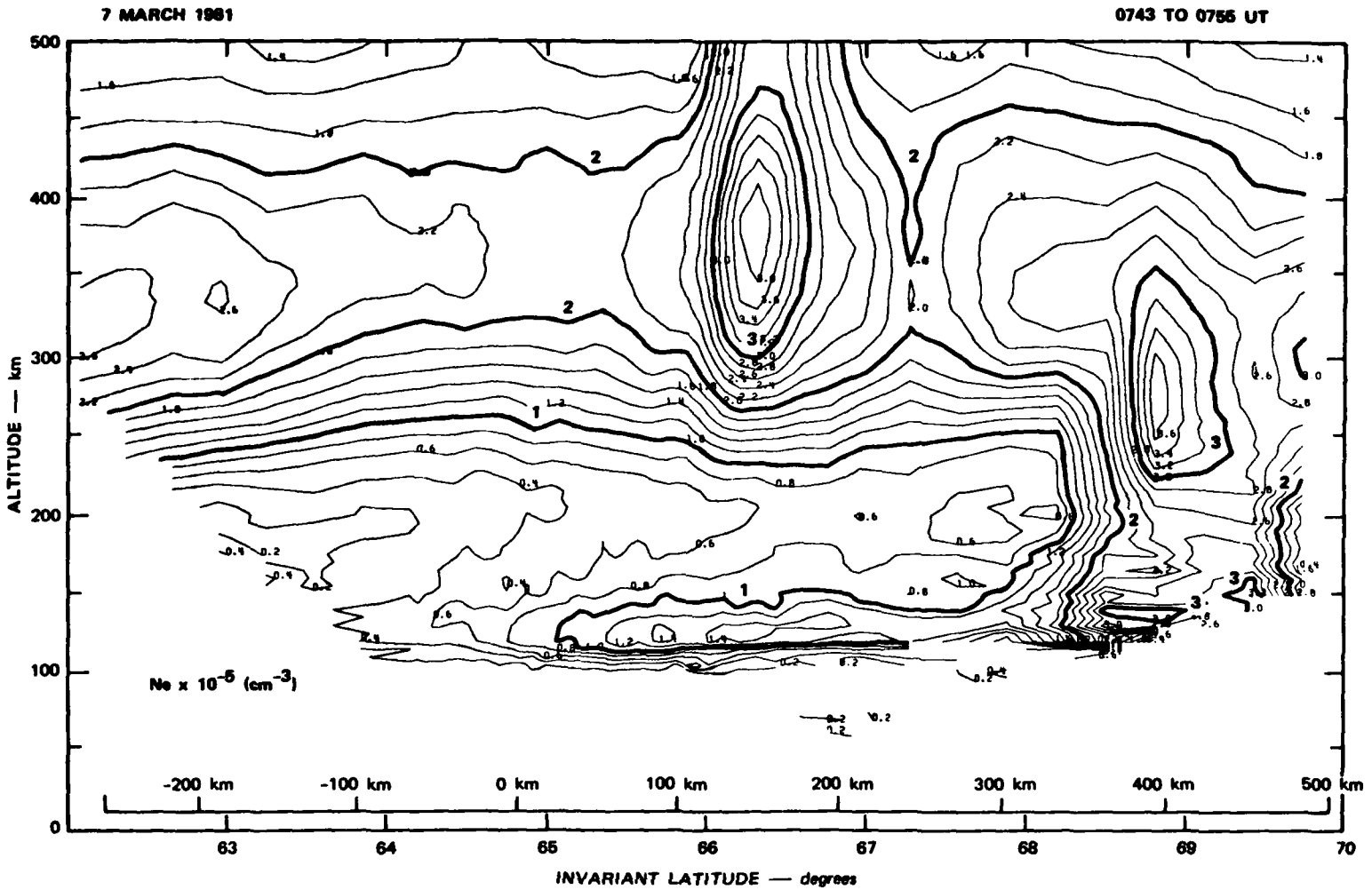

FIGURE 6 ELECTRON-DENSITY CONTOUR PLOT: 0743 TO 0755 UT

large spatial gradients. According to this definition, the equatorward boundary of the diffuse aurora in Figure 4 is at about 69.5°. In Figure 5, this boundary has moved to 67° and in Figure 6 it is at 65°. In Figure 6, a local maximum in density is apparent between 66° and 67°. North of this maximum the ionization falls off slightly. Then at 68°, a more structured enhancement with densities of about 3×10^5 el/cm^3 appears. The ionization pattern in Figure 6 is typical of that usually seen in the evening sector auroral zone; i.e., the diffuse aurora contains one primary electron density maximum, which is often localized in latitude. Auroral arcs are often found north of this enhancement and separated from it by a dark band within which the ionization is depleted [Robinson et al., 1981].

Figure 7 shows the conductivity, electric field and current profile for this scan. The height-integrated Hall and Pederson conductivities are nearly equal and do not exceed 6 mhos. The zonal component of the electric field is small, but the meridional component is large and northward. A poleward gradient is present in the electric field overhead. This produces a poleward gradient in the northward current, which implies the presence of downward field-aligned current at the southern edge of the diffuse aurora.

Just after deployment of the AFGL aircraft (0740 UT) the radar scanned twice in azimuth to the east. The electric fields computed from the azimuth scan are shown in Figures 8 and 9. The fields are somewhat smaller than those measured during the elevation scan, which ended at 0755 UT. This discrepancy might be caused by longitudinal variations in the electric field since in the azimuth scan mode the measurements are made approximately 400 km to the east (30 min of local time). Another possibility is that the presence of E region neutral winds have biased the elevation scan measurements.

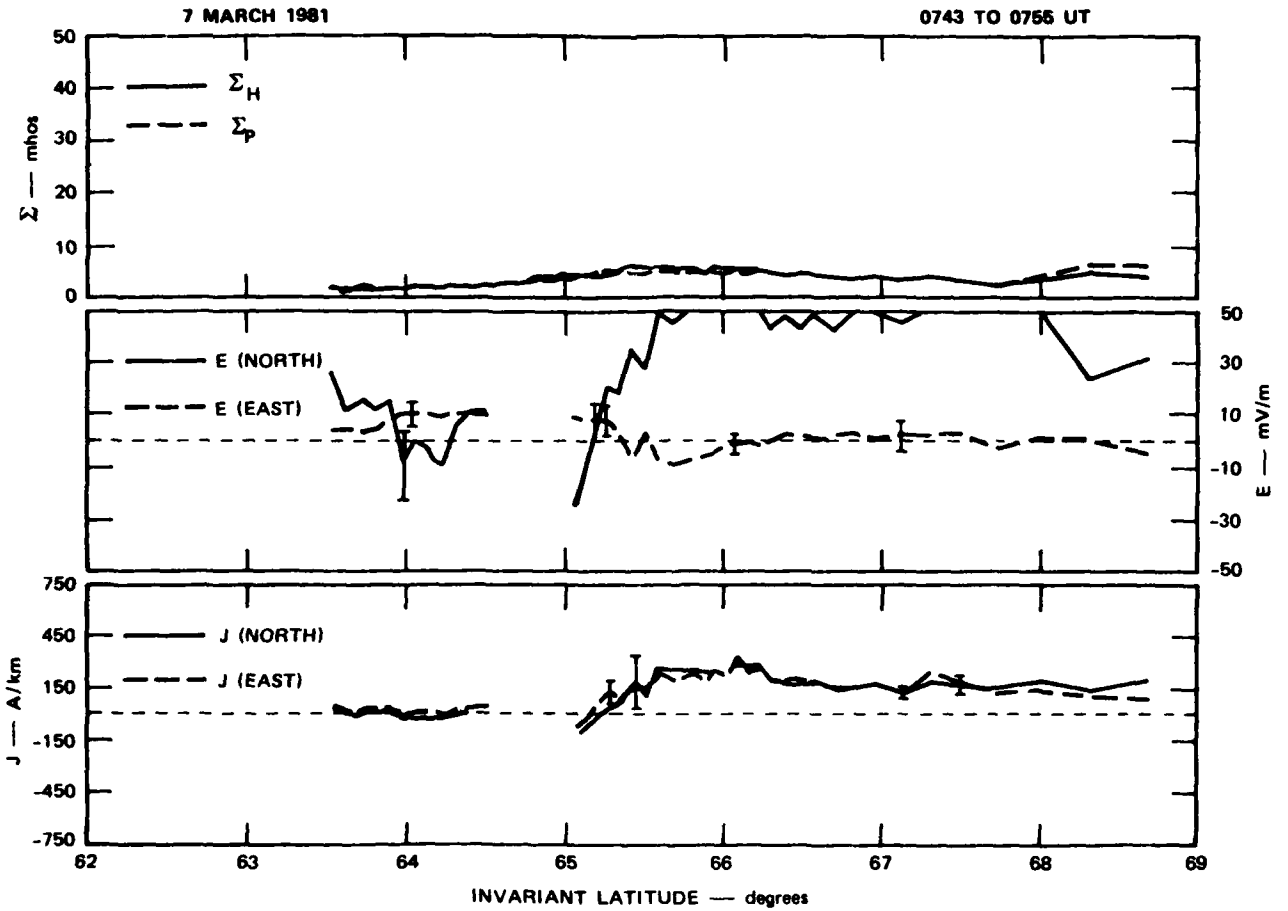

FIGURE 7 HEIGHT-INTEGRATED CONDUCTIVITIES, ELECTRIC FIELDS AND CURRENTS COMPUTED FROM RADAR DATA OBTAINED DURING MERIDIAN SCAN OF FIGURE 6

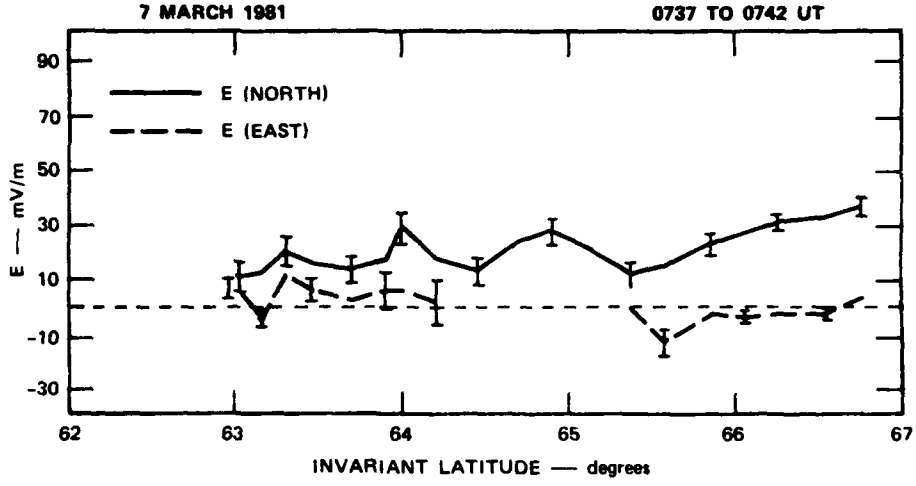

FIGURE 8 ELECTRIC FIELDS COMPUTED FROM AZIMUTH-SCAN DATA: 0737 TO 0742 UT. The eastward electric field is obtained from the preceding elevation scan.

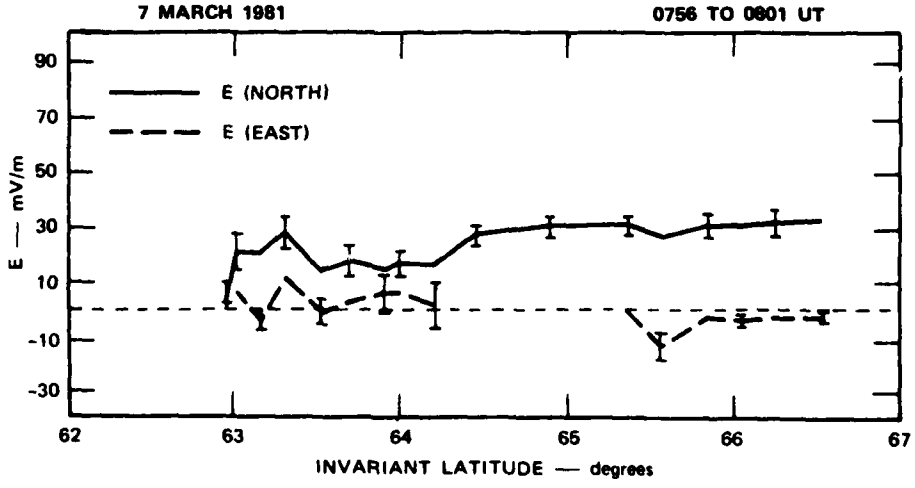

FIGURE 9 ELECTRIC FIELDS COMPUTED FROM AZIMUTH-SCAN DATA: 0756 TO 0801 UT. The eastward electric field is the same as in Figure 8.

B. Radar Measurements From 0803 to 0834 UT

At 0803 UT, the radar operating mode was changed so that the antenna scanned in the north within the region spanned by the rocket trajectories. During the time that the first three rockets were launched, the radar made seven consecutive partial elevation scans in the north. Expanded plots for these seven scans are shown in Figures 10 through 16. The rocket echoes in these scans have been eliminated by rejecting specific radar records. The locations of these echoes are indicated in the contour plots by shaded circles. The trajectories of the first three payloads have been added to Figures 11, 12, 15, and 16. The trajectories are not parabolic because of the geomagnetic coordinate system used in the plots.

Figures 17 through 19 show three electron density profiles obtained at selected times during the rocket launches. Attempts have been made to choose profiles free from rocket-echo contamination and as close as possible to the points of apogee of the payloads. The locations of the profiles are shown by vertical lines in Figures 10, 13, and 16. The profiles all peak at about 125-km altitude in the E region with maximum densities of 1.5 to 2 x 10^5 el/cm^3. The similarity between the three is evidence for the temporal and spatial uniformity of the diffuse aurora during the flights.

C. Radar Measurements From 0849 to 0950 UT

After reentry of the third rocket the radar operating mode was switched to a fixed-position mode. At 0849 UT, when data recording was resumed, the diffuse aurora was still overhead. Electron-density profiles for the first three fixed-position dwells are shown in Figure 20. The five consecutive fixed-position measurements were used to compute three values of the electric field and E-region neutral winds. These measurements are shown in Table 4. The electric-field measurements agree well with those made earlier in the azimuth scan mode. The northward electric field at 65° was 27 mV/m, which agrees well with the 30 mV/m measured in the three-position mode. At 0900 UT, the electric field had a slightly larger westward component of 5 mV/m.

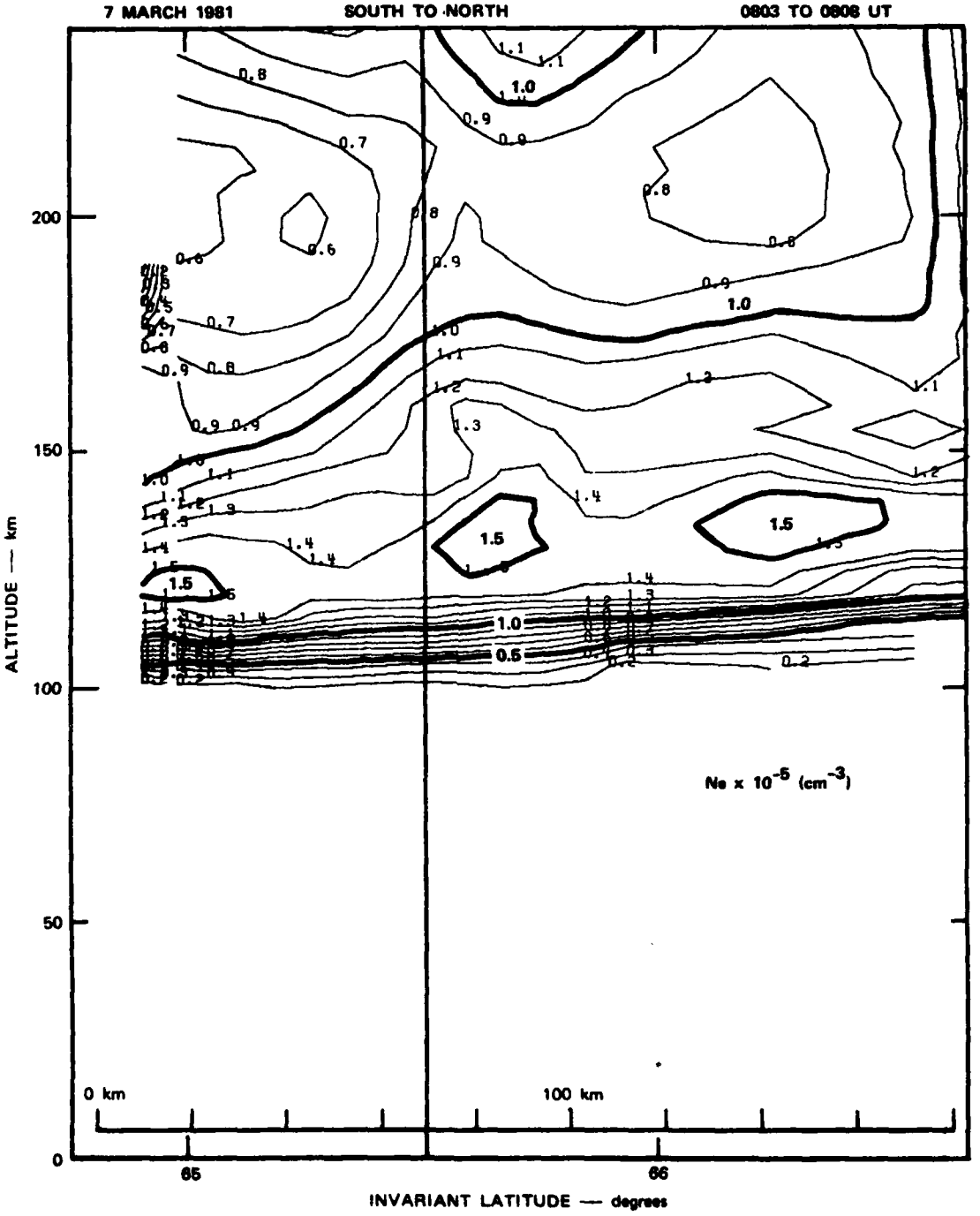

FIGURE 10 EXPANDED VIEW OF ELECTRON-DENSITY-CONTOUR PLOT CONSTRUCTED FROM PARTIAL MERIDIAN SCAN BEGINNING AT 0803 UT. No rocket echoes were present in this scan. An electron-density profile along the vertical line is shown in Figure 17.

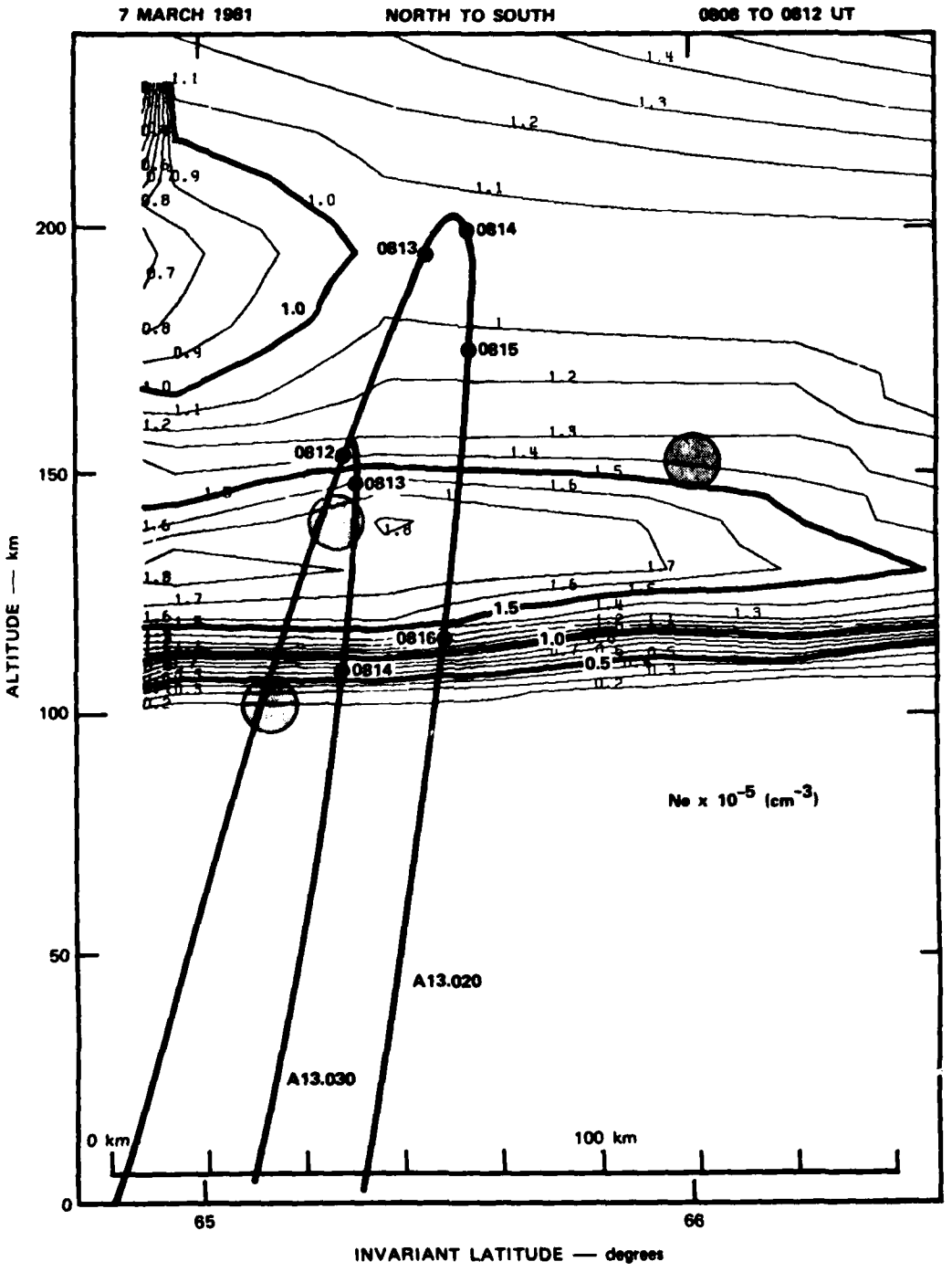

FIGURE 11 EXPANDED VIEW OF ELECTRON-DENSITY-CONTOUR PLOT CONSTRUCTED FROM PARTIAL MERIDIAN SCAN BEGINNING AT 0808 UT. The locations of several rocket echoes are shown by the shaded circles. These data were eliminated in constructing the contours. The heavy lines represent the trajectories of Rockets A13.030 (Rocket 1) and A13.020 (Rocket 2) in geomagnetic coordinates.

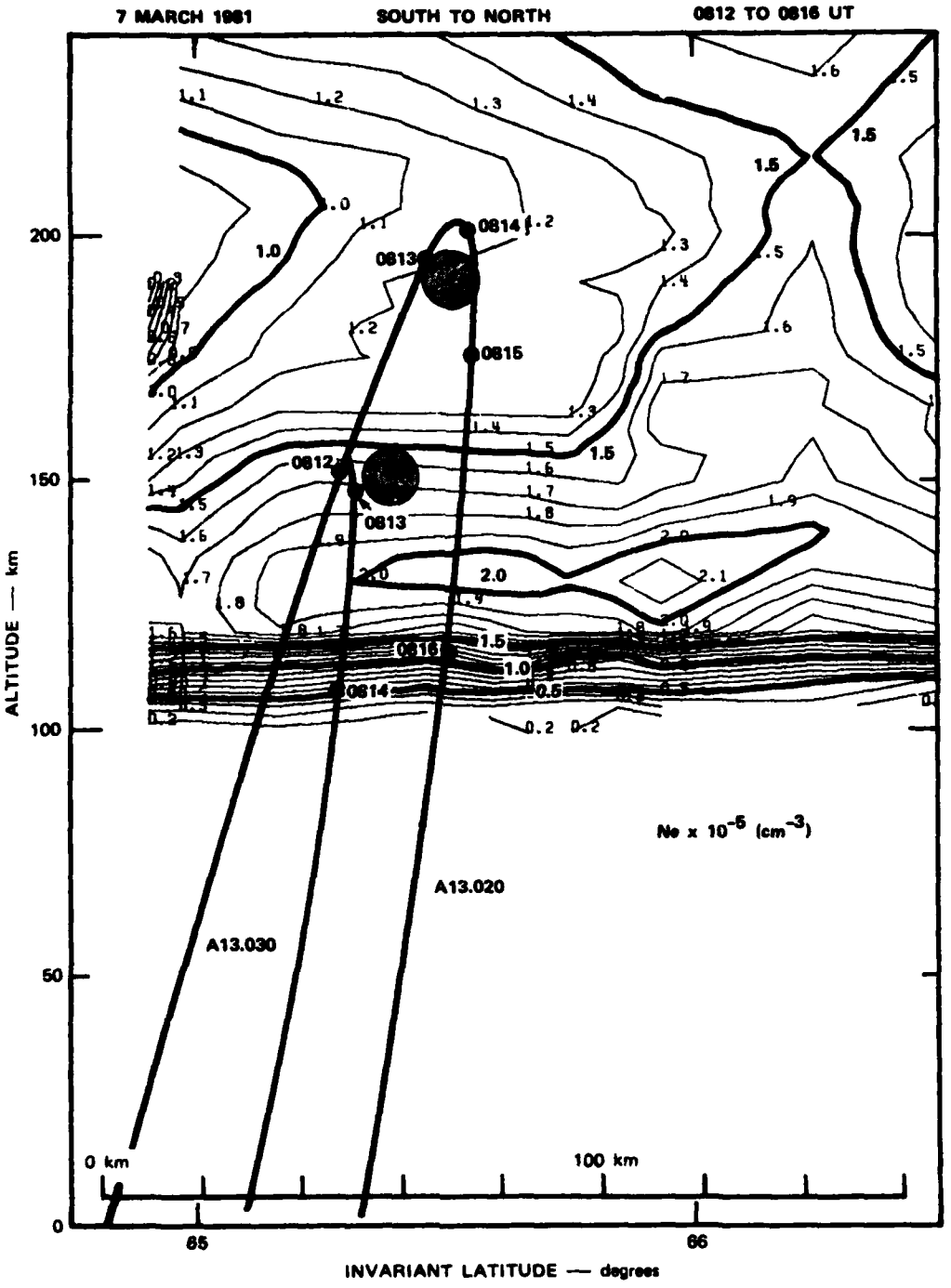

FIGURE 12 EXPANDED VIEW OF ELECTRON-DENSITY-CONTOUR PLOT CONSTRUCTED FROM PARTIAL MERIDIAN SCAN BEGINNING AT 0812 UT. The locations of rocket echoes are shown by the shaded circles. Trajectories of Rockets A13.030 (Rocket 1) and A13.020 (Rocket 2) are shown.

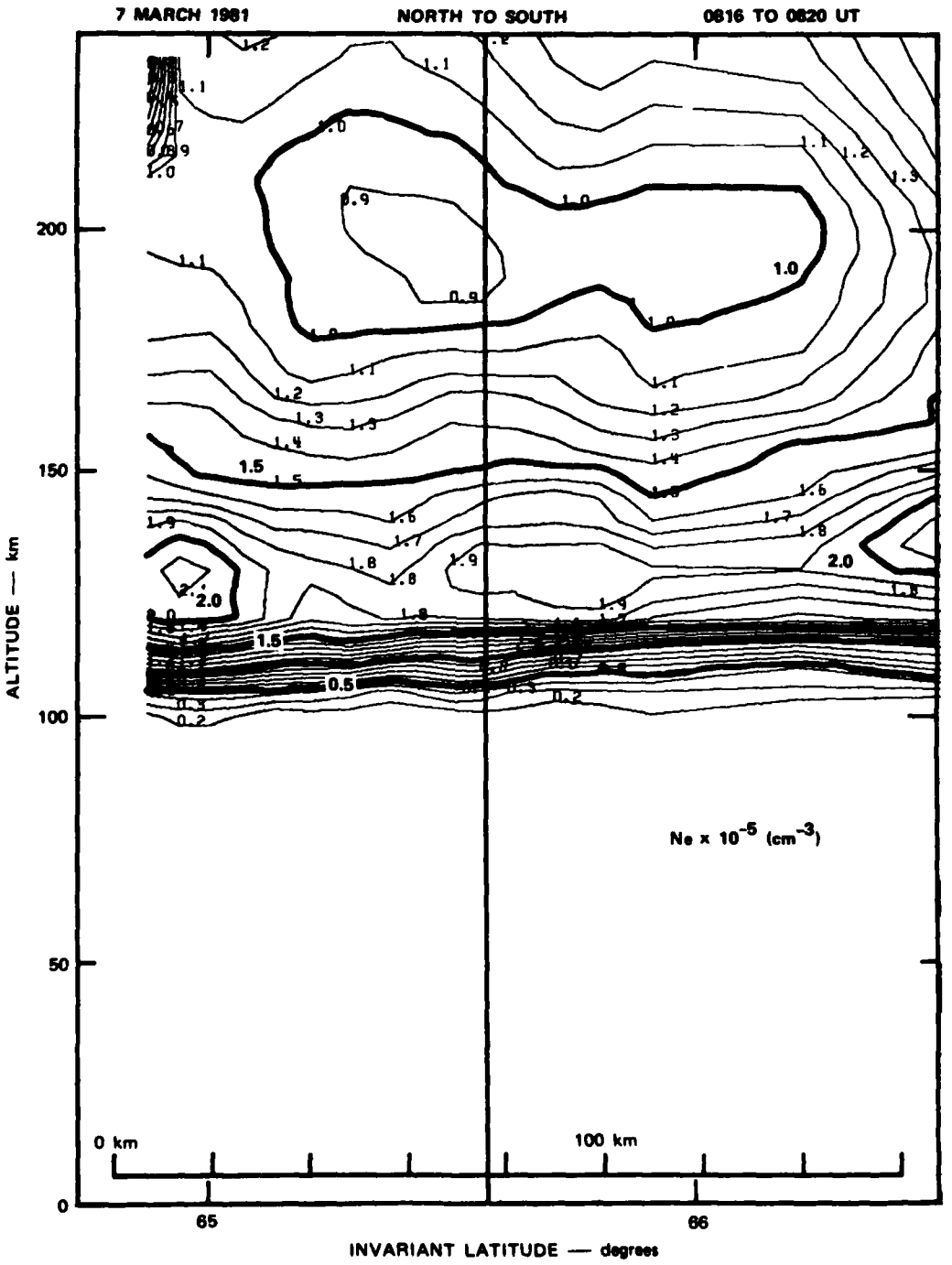

FIGURE 13 EXPANDED VIEW OF ELECTRON-DENSITY-CONTOUR PLOT CONSTRUCTED FROM PARTIAL MERIDIAN SCAN BEGINNING AT 0816 UT. No rocket echoes were present in this scan. An electron-density profile along the vertical line is shown in Figure 18.

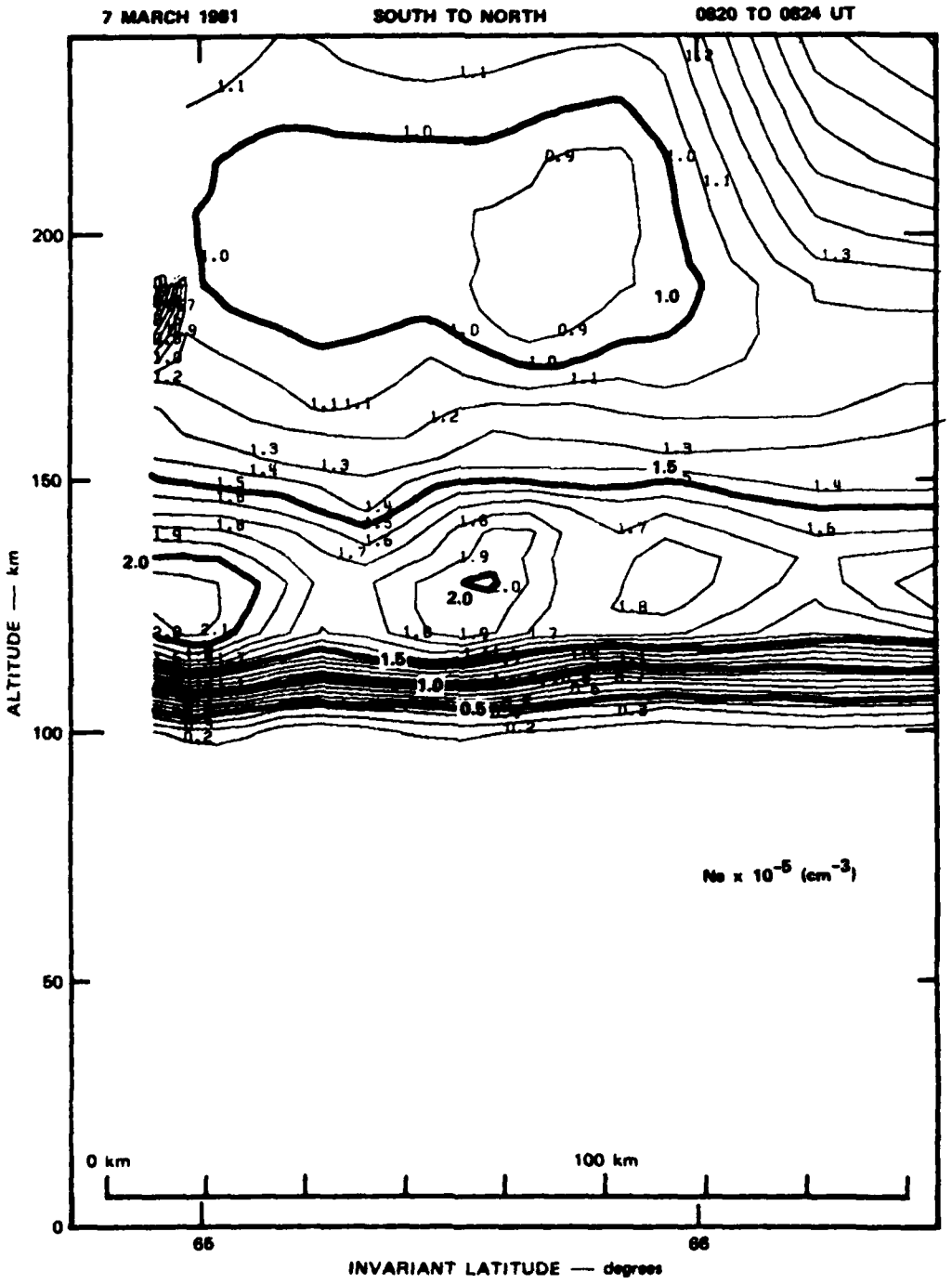

FIGURE 14 EXPANDED VIEW OF ELECTRON-DENSITY-CONTOUR PLOT CONSTRUCTED FROM PARTIAL MERIDIAN SCAN BEGINNING AT 0820 UT. No rocket echoes were present in this scan.

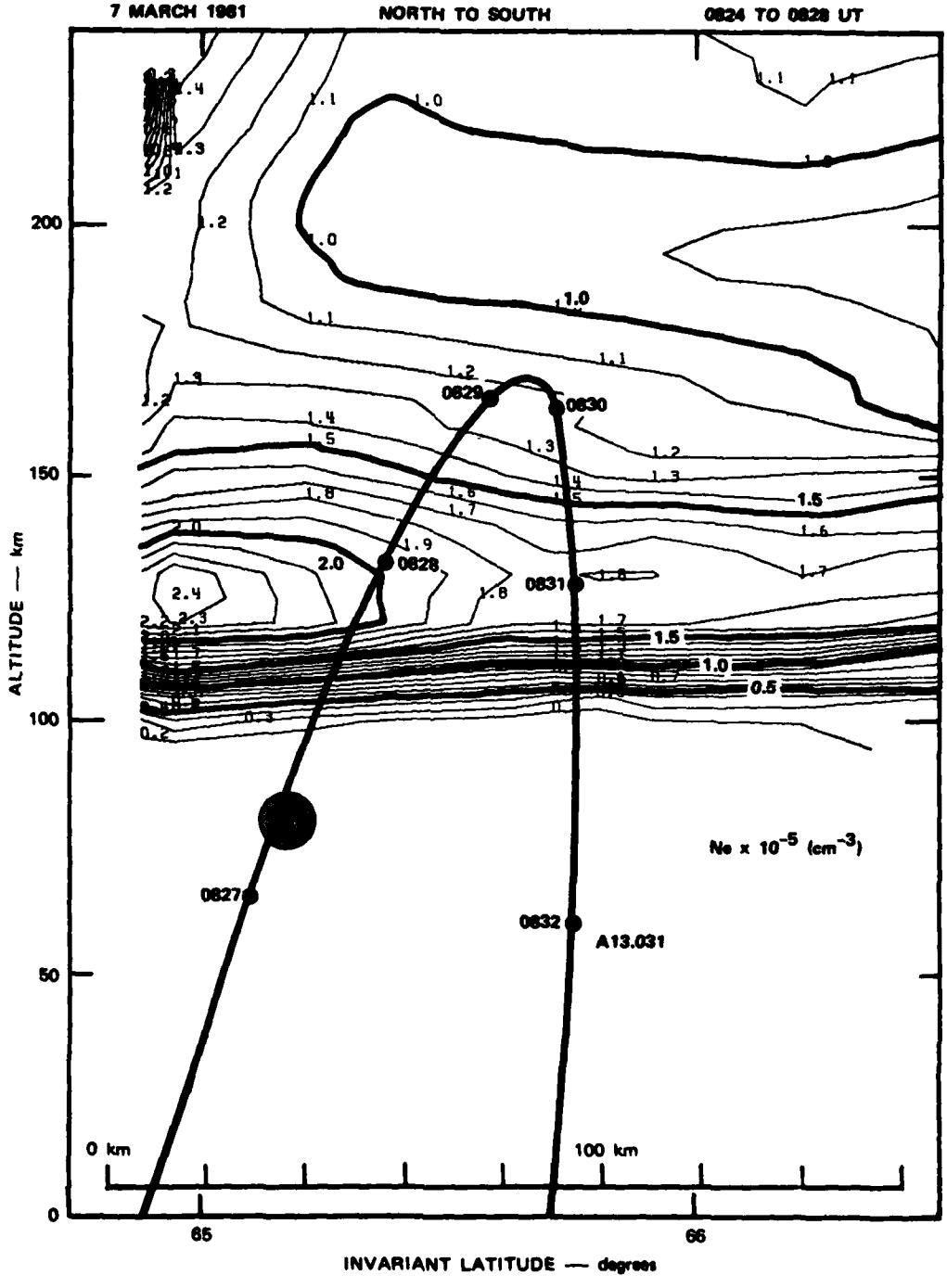

FIGURE 15 EXPANDED VIEW OF ELECTRON-DENSITY-CONTOUR PLOT CONSTRUCTED FROM PARTIAL MERIDIAN SCAN BEGINNING AT 0824 UT. The trajectory of Rocket A13.031 (Rocket 3) is shown.

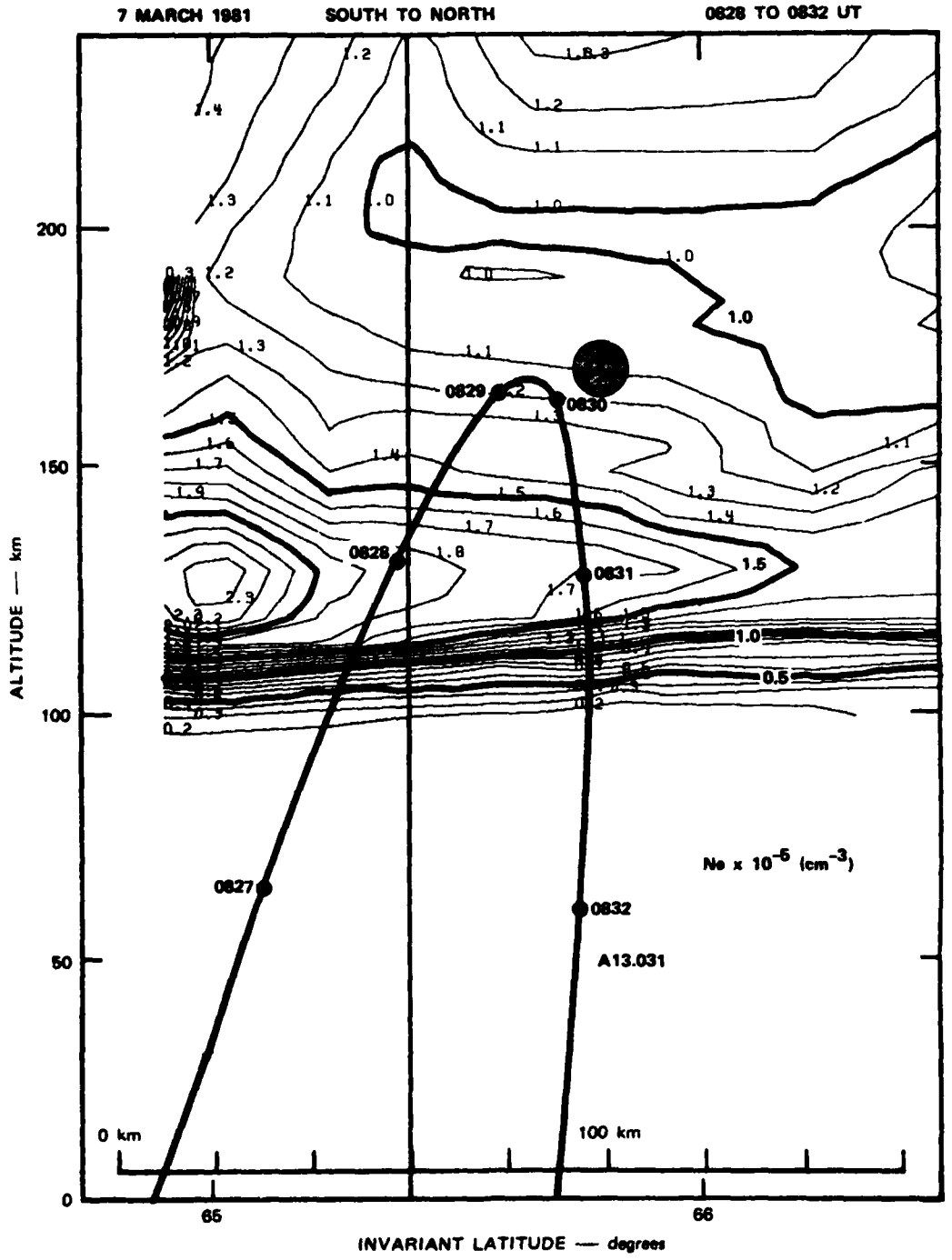

FIGURE 16 EXPANDED VIEW OF ELECTRON-DENSITY-CONTOUR PLOT CONSTRUCTED FROM PARTIAL MERIDIAN SCAN BEGINNING AT 0828 UT. An electron-density profile along the vertical line is shown in Figure 19.

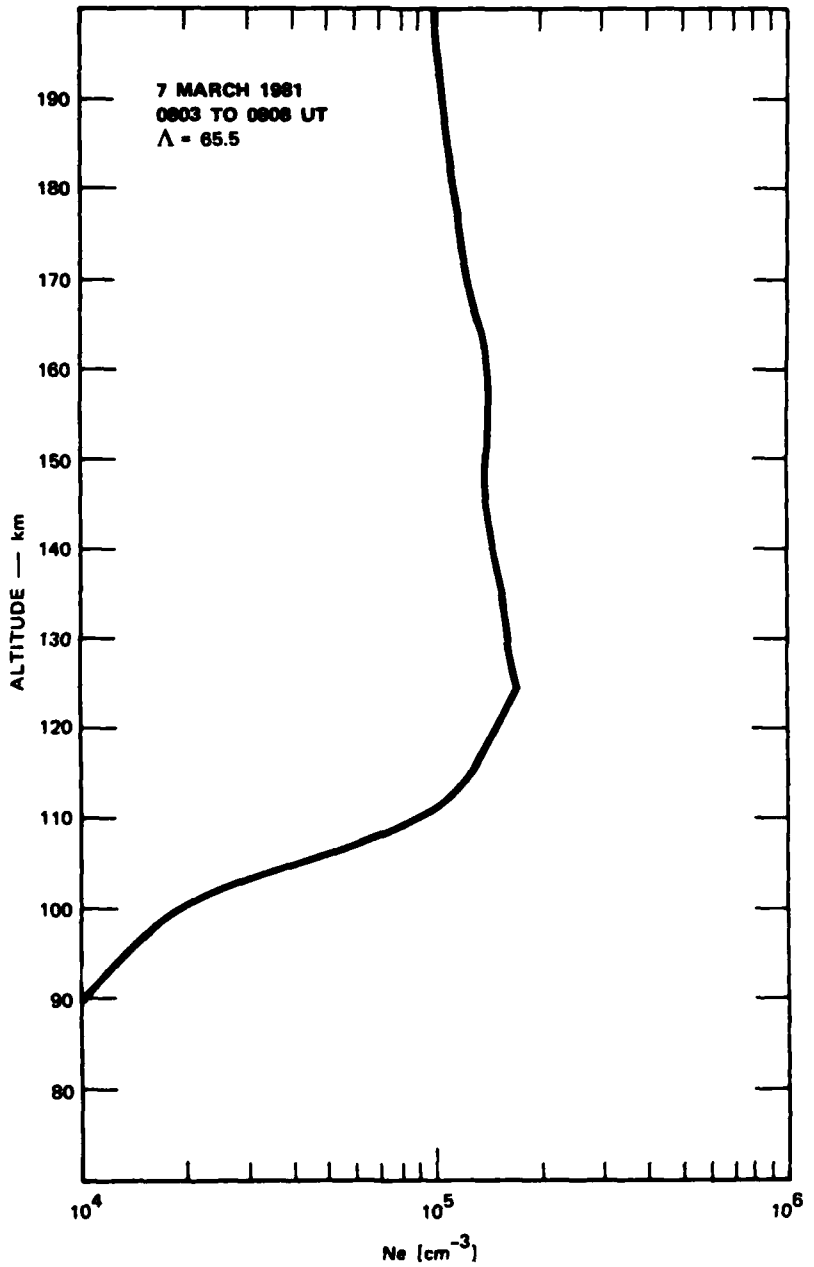

FIGURE 17 ELECTRON DENSITY AS A FUNCTION OF ALTITUDE ALONG A MAGNETIC-FLUX TUBE. The location of the flux tube is given by the vertical line in Figure 10.

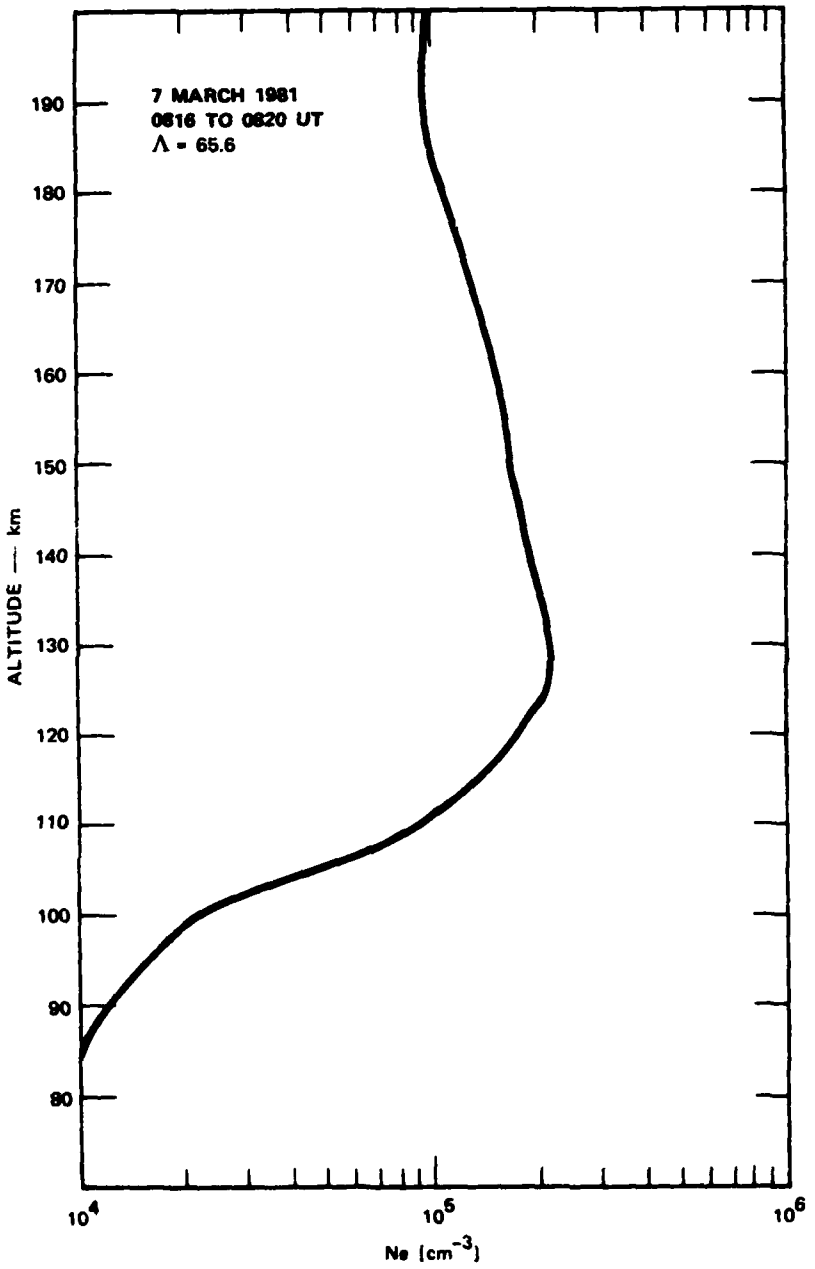

FIGURE 18 ELECTRON DENSITY AS A FUNCTION OF ALTITUDE ALONG A MAGNETIC-FLUX TUBE. The location of the flux tube is given by the vertical line in Figure 13.

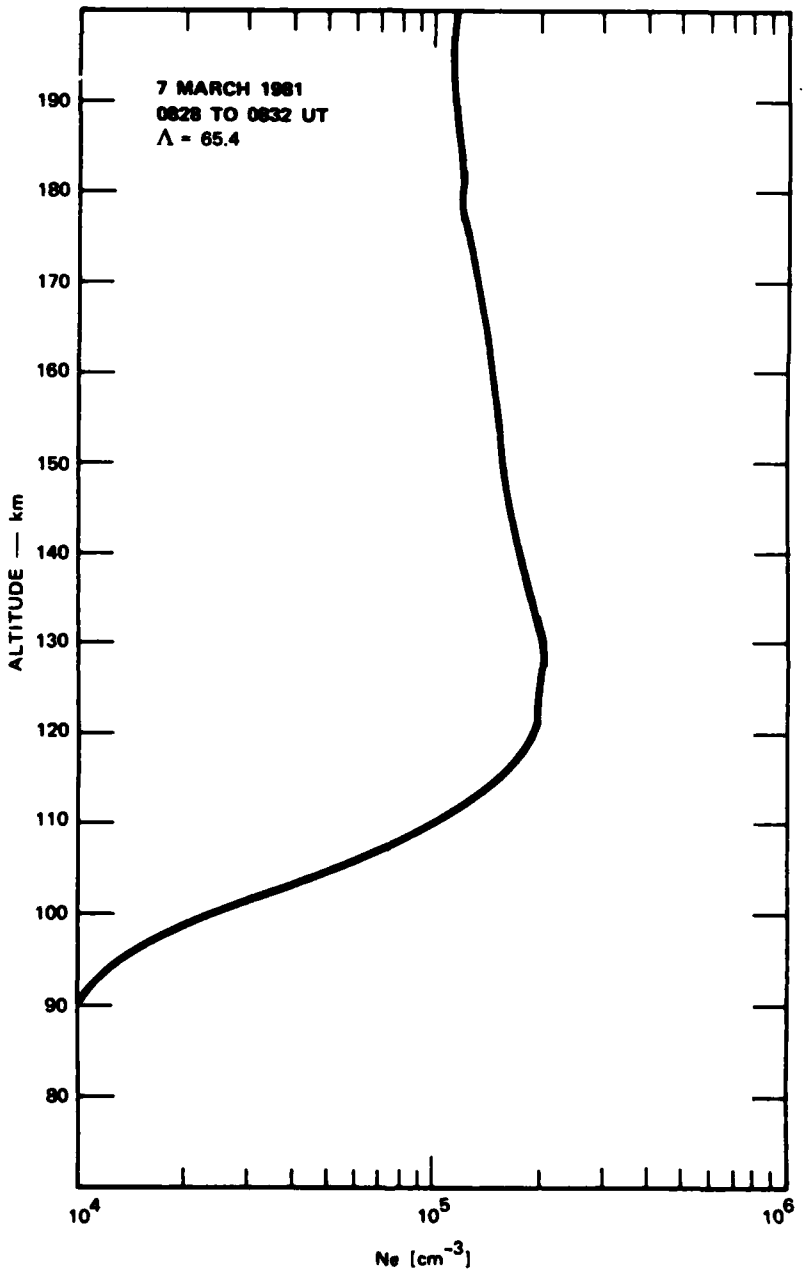

FIGURE 19 ELECTRON DENSITY AS A FUNCTION OF ALTITUDE ALONG A MAGNETIC-FLUX TUBE. The location of the flux tube is given by the vertical line in Figure 16.

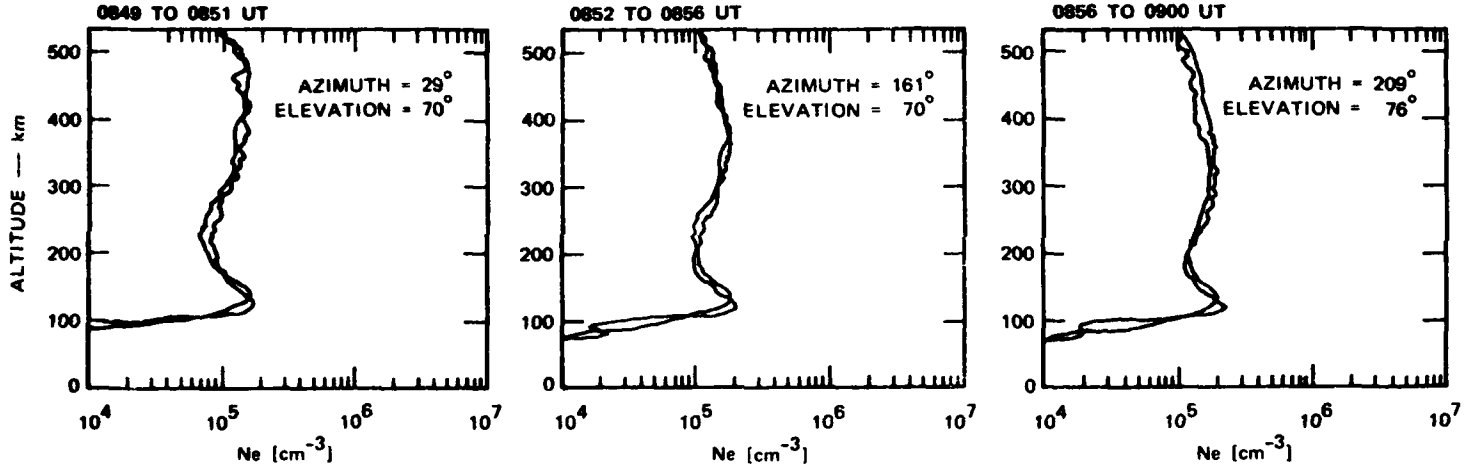

FIGURE 20 ELECTRON DENSITY AS A FUNCTION OF ALTITUDE ALONG THE RADAR LINE OF SIGHT FOR FIRST THREE FIXED-POSITION DWELLS. *Profiles from long- and short-pulse returns are shown.*

Table 4

FIXED-POSITION ELECTRIC-FIELD AND
NEUTRAL WIND MEASUREMENTS

Time (UT)	E-East (mV/m)	E-North (mV/m)	U-East (m/s)	U-North (m/s)
0849-0900	-3.22	28.94	72	7
0852-0904	-5.63	29.02	-10	-61
0856-0909	-5.63	28.70	58	-90

Electron density data from an elevation scan made between 0912 UT and 0925 UT are shown in Figure 21. This scan was made while the AIO aircraft was between Fort Yukon and Chatanika flying southward along the magnetic meridian. The contour plot shows that by this time the diffuse aurora stretched far to the south and was uniform except for several minor enhancements between 64° and 66°.

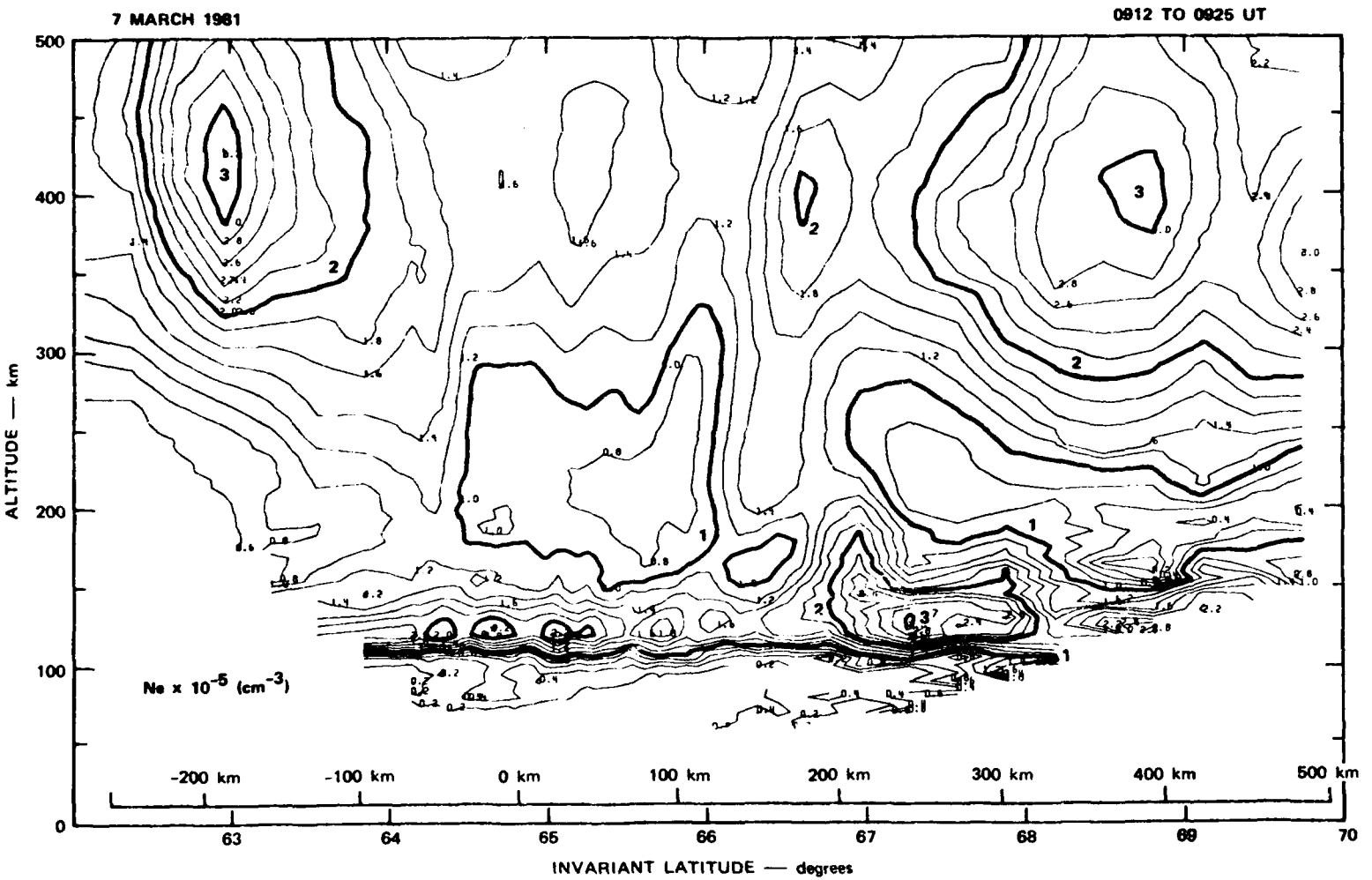

FIGURE 21 ELECTRON-DENSITY CONTOUR PLOT CONSTRUCTED FROM MERIDIAN SCAN BEGINNING AT 0912 UT

V DISCUSSION

The electron density measurements during the evening of 7 March 1981 are summarized by the gray-shaded plot of Figure 22. Here the electron density at 125 km is plotted as a function of latitude and UT. The southward advance of the ionization is apparent in this figure. This apparent motion is probably a result of the earth's rotation beneath a fixed pattern that is aligned along the auroral oval. In the evening sector, the invariant latitude of the equatorward edge of the auroral oval is a function of local time. The dark line in Figure 22 shows the approximate position of the equatorward edge of the diffuse aurora as defined by an electron density of 1×10^5 el/cm^3. The average slant of this line is consistent with the shape of the statistical auroral oval (Gussenhoven et al., 1981). This agreement indicates that the oval was quite steady during the evening with no obvious variations in size or shape. The position of the equatorward edge of the diffuse aurora is the same as the equatorward edge of the Q=5 auroral oval [Feldstein, 1967]; [Whalen, 1970].

The electric-field measurements are summarized in Figure 23. Here we have plotted the F-region E x B drift velocity as a function of invariant latitude and time. The measurements from each scan are plotted as vectors at a time corresponding to the middle of the scan. However, the scans required 4 to 12 min to complete, so that the measurements in any one scan are not made at the same time. The dashed vectors between 0854 and 0906 UT represent the three fixed-position measurements. These vectors are placed at an invariant latitude of 65°, though they actually represent spatially averaged drift measurements over the area shown within the three dashed circles in Figure 3. The dominance of the westward drift (northward electric field) throughout the evening is apparent in this figure.

Both the density and electric fields observed are consistent with those typically seen in the evening diffuse aurora. The absence of

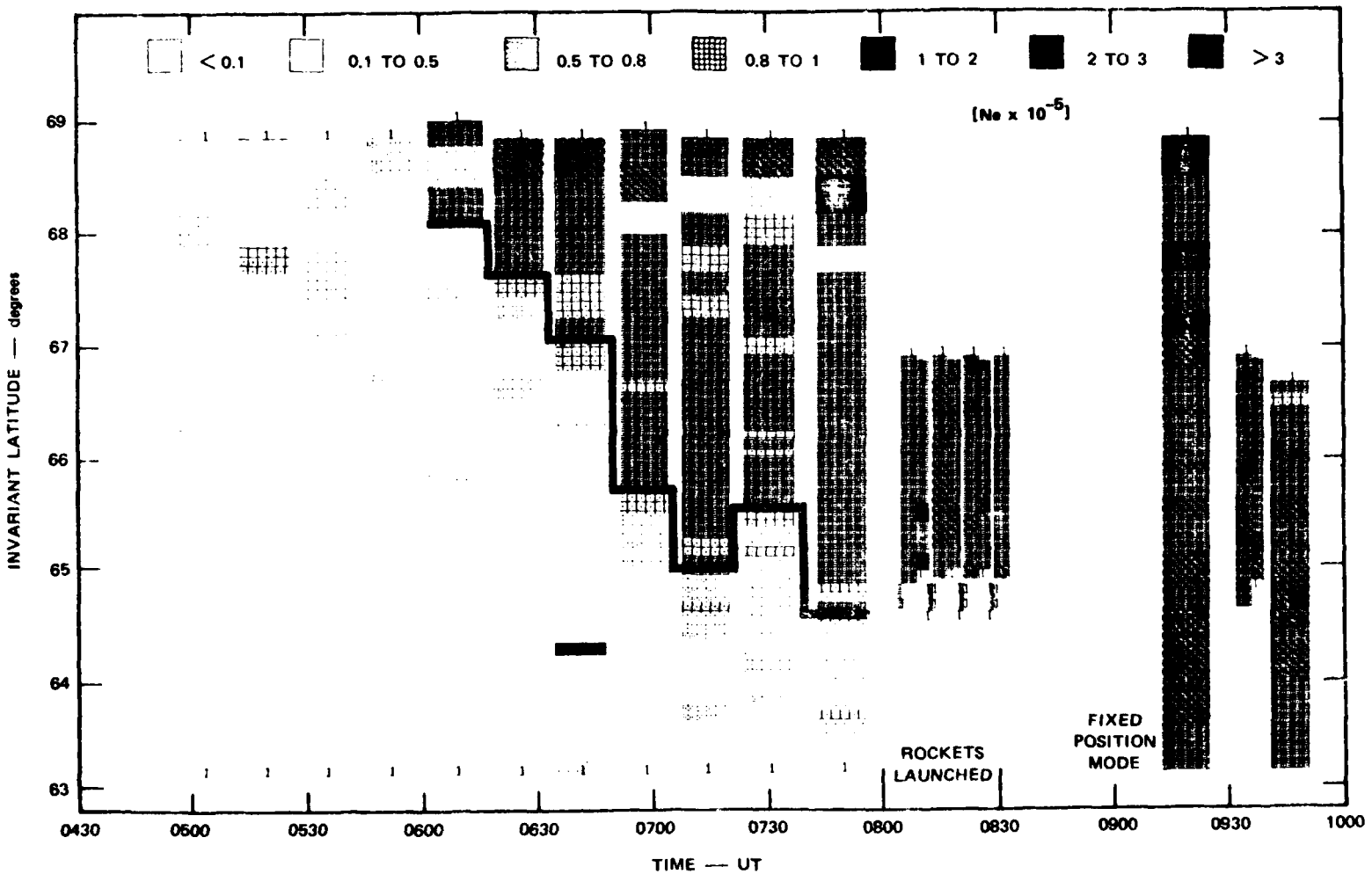

FIGURE 22 GREY SHADE PLOT SHOWING ELECTRON DENSITY AT AN ALTITUDE OF 125 km AS A FUNCTION OF INVARIANT LATITUDE AND UT. *Regions with densities above* 10^5 *el/cm*^{3} coincide with the diffuse aurora.

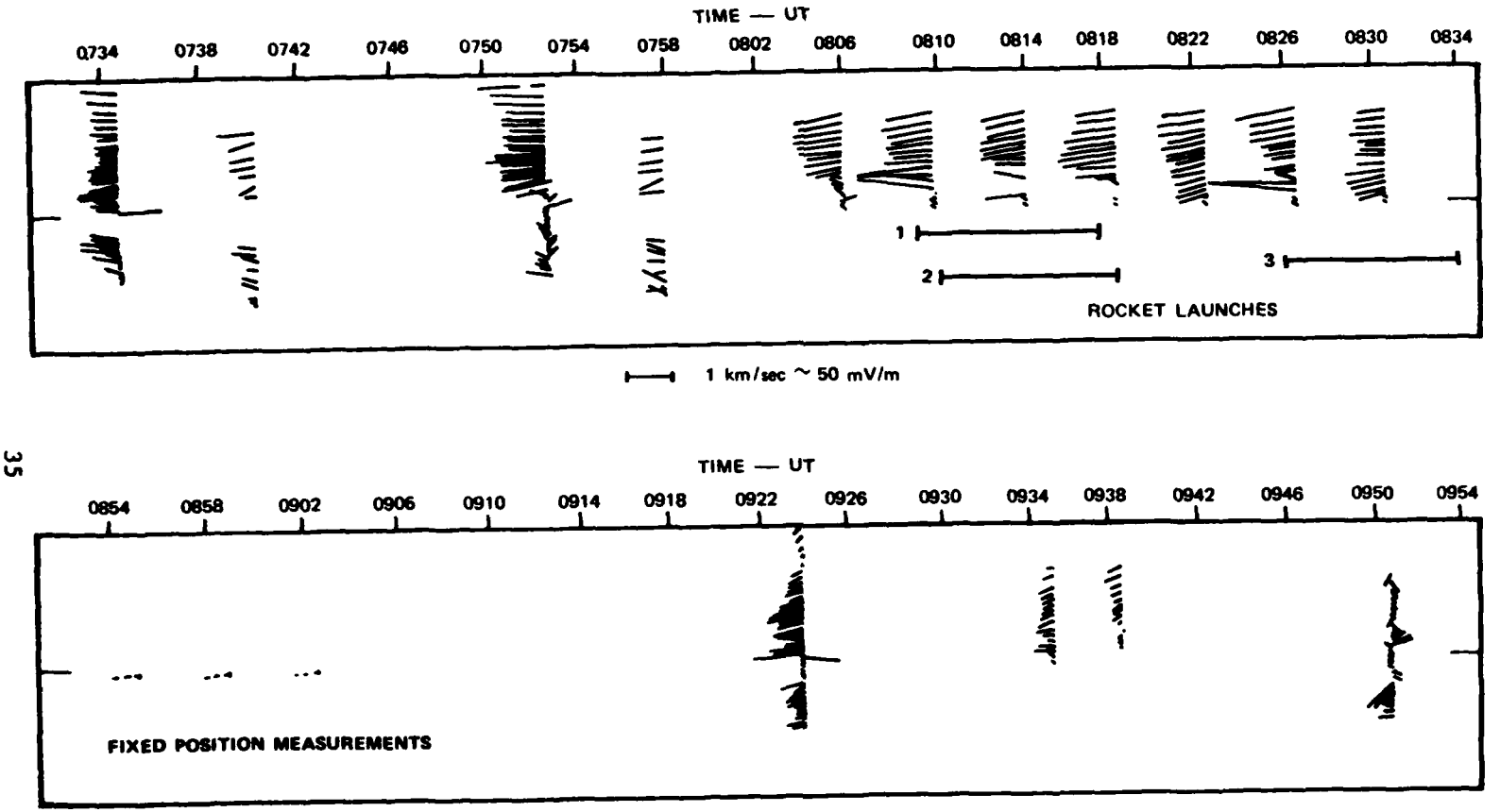

FIGURE 23 VECTOR DIAGRAM OF F-REGION DRIFT VELOCITY AS A FUNCTION OF INVARIANT LATITUDE AND UT. The direction of the electric field can be obtained by rotating the vectors clockwise by 90°. Three fixed-position electric-field measurements are shown at lower left.

discrete enhancements in electron density and the small magnetic perturbations recorded by the ground-based magnetometers indicate that auroral activity on this night was quiet to moderate.

Information about the particle precipitation producing the diffuse aurora can be deduced from the electron density profiles. The method has been outlined by Vondrak and Baron [1977]. The density profile is converted to a production rate q(h) according to

$$q(h) = \alpha n^2$$

where α is the height-dependent recombination rate and n is the electron density. The production profile is deconvolved to yield the flux of electrons as a function of energy between 1 keV and 150 keV. This is done by starting with the lowest altitudes (highest energies) and working upward (downward in energy). The computed spectra for the three profiles shown earlier (Figures 17 to 19) are plotted on the right hand side of Figures 24 through 26. The solid line is a plot of log F(E) as a function of log E (left hand and lower scales). The dashed line plots log F(V) as a function of E (right hand and upper scales). As a check on the calculations, these energy distributions were used to recompute the electron density profiles (circles in the left hand plots) for comparison with the measured profiles (solid lines on right). The derived spectra are Maxwellian with mean energies of about 2 keV (characteristic energies of 1 keV). These energies are typical of plasma sheet particles. The energy flux associated with the precipitation is 1.0 to 2.0 ergs/cm^2-s.

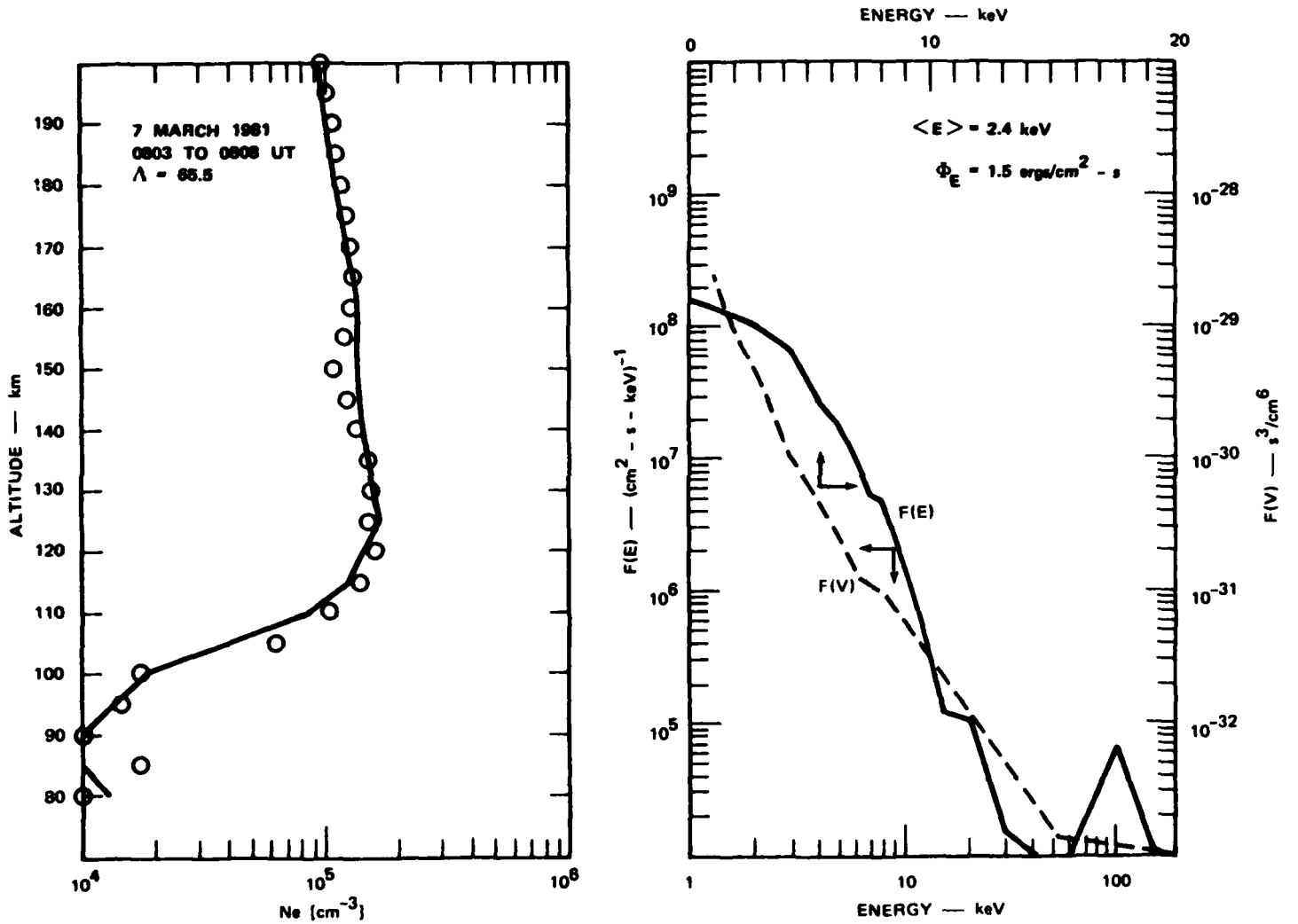

FIGURE 24 ELECTRON-ENERGY SPECTRUM DEDUCED FROM RADAR MEASURED DENSITY PROFILES. Solid curve at left is the same as Figure 17. Circles at left represent the density profile computed from the inferred energy spectrum.

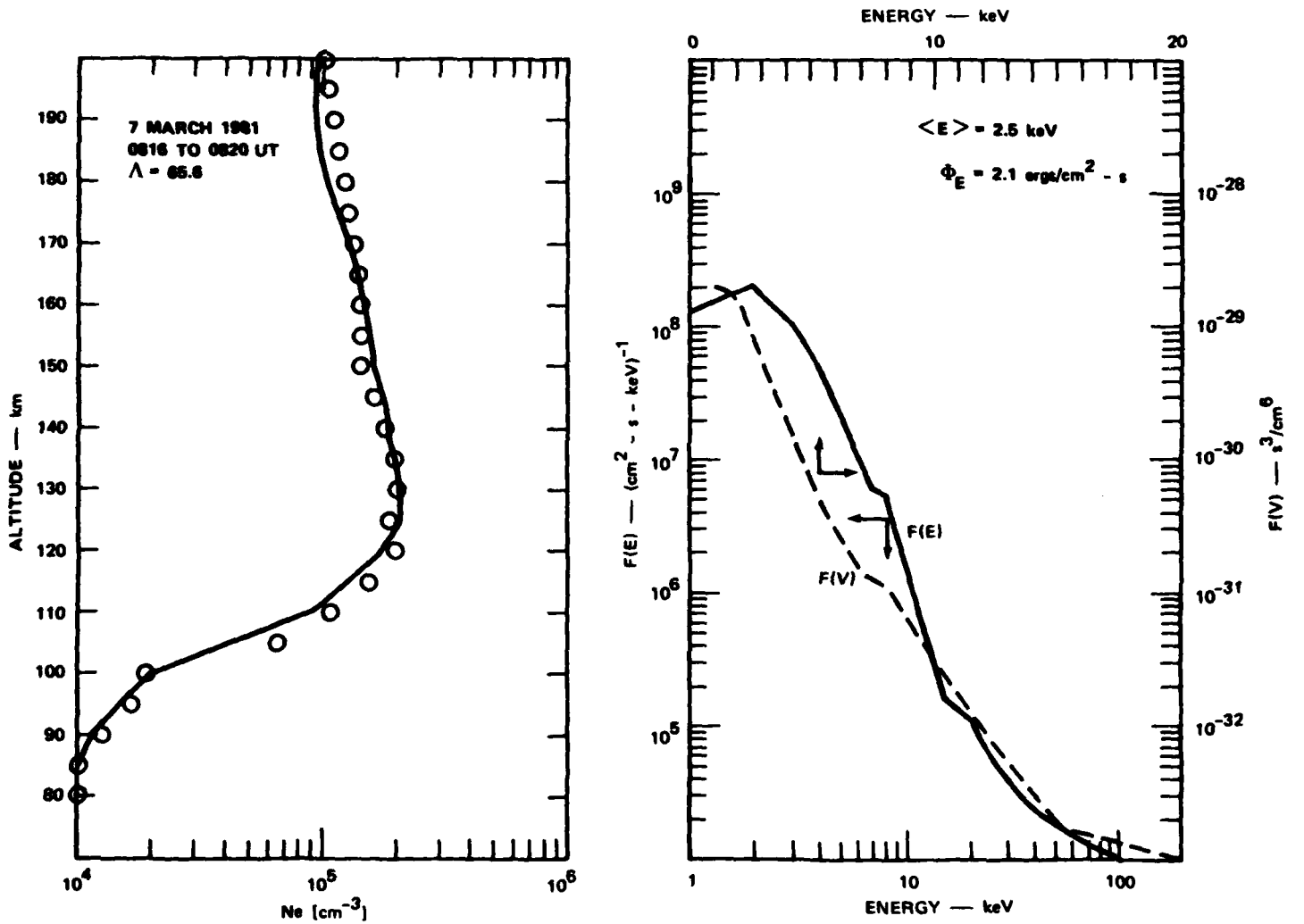

FIGURE 25 ELECTRON-ENERGY SPECTRUM DEDUCED FROM RADAR MEASURED DENSITY PROFILES. Solid curve at left is the same as Figure 18. Circles at left represent the density profile computed from the inferred energy spectrum.

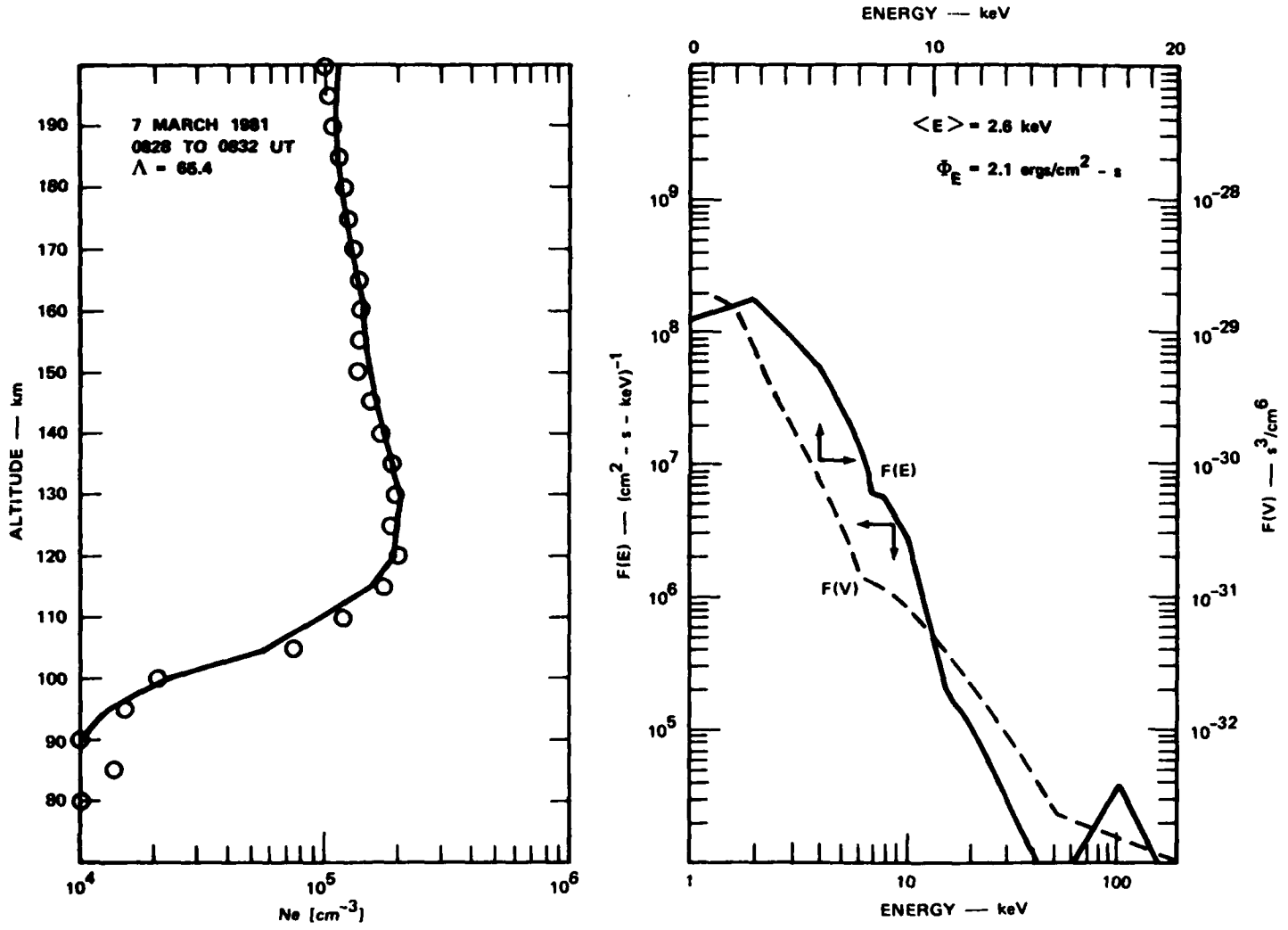

FIGURE 26 ELECTRON-ENERGY SPECTRUM DEDUCED FROM RADAR MEASURED DENSITY PROFILES. Solid curve at left is the same as Figure 19. Circles at left represent the density profile computed from the inferred energy spectrum.

VI CONCLUSION

The radar measurements have shown that auroral conditions during the launch of the four AFGL rockets were quiet to moderate. The southward advance of the diffuse aurora during the evening was consistent with the average quiet time shape of the auroral oval. Electric fields were predominantly northward. No reversals in the field were observed indicating that the Harang discontinuity was well to the east. Electron-density measurements showed no discrete structures within the limits of the rocket trajectories. Electron-density profiles beneath the rocket trajectories could be accounted for by local production due to electrons with energy distributions typical of plasma sheet particles. The characteristics of the precipitation did not change during the time the four rockets were launched. Thus, the launch criteria appear to have been satisfied and the ground-based and in-situ measurements should provide an excellent data base with which to test the theoretical models.

REFERENCES

Baron, M. J., "The Chatanika Radar System," in Radar Probing of the Auroral Plasma Proceedings of the EISCAT Summer School, Tromsø Norway, June 5-13, 1975, A. Brekke, ed., pp. 103-141 (Universitetsforlaget, Tromsø-Oslo-Bergen, 1977).

de la Beaujardiere, O., V. Wickwar, C. Leger, M. McCready, and M. Baron, "The Software System for the Chatanika Incoherent-Scatter Radar," Project 8358, SRI International, Menlo Park, CA (November, 1980).

de la Beaujardiere, O., R. Vondrak, R. Heelis, W. Hanson, and R. Hoffman, "Auroral Arc Electrodynamic Parameters Measured by AE-C and the Chatanika Radar," J. Geophys. Res., in press, 1981.

Feldstein, Y. I., and G. V. Starkov, "Dynamics of Auroral Belt and Polar Geomagnetic Disturbances," Planet. Sp. Sci., 15, 209-229 (1967).

Gussenhoven, M. S., D. A. Hardy, and W. J. Burke, "DMSP/F2 Electron Observations of Equatorward Auroral Boundaries and Their Relationship to Magnetospheric Electric Fields," J. Geophys. Res., 86, 768-778 (1981).

Jacchia, L. J., "Static Diffusion Models of the Upper Atmosphere with Empirical Temperature Profiles," Smithsonian Contrib. Astrophys., 8, 215-257 (1965).

Rino, C. L., M. J. Baron, G. H. Burch, and O. de la Beaujardiere, "A Multipulse Correlator Design for Incoherent Scatter Radar," Radio Sci., 9, 1117-1127 (1974).

Robinson, R. M., R. R. Vondrak, and T. A. Potemra, "Ionospheric Conductivities and Field-Aligned Currents Associated with Evening-Sector Auroral Arcs," Abstract of paper presented at Spring Meeting of American Geophysical Union, EOS, 62 (1981).

Vondrak, R. R., and M. J. Baron, "A Method of Obtaining the Energy Distribution of Auroral Electrons from Incoherent Scatter Energy Measurements," in Radar Probing of the Auroral Plasma, Proceedings of the EISCAT Summer School, Tromsø, Norway, June 5-13, 1975, A. Brekke, ed., pp. 315-330, (Universitetsforlaget, Tromsø-Oslo-Bergen, 1977).

Whalen, J. A., "Auroral Oval Plotter and Nomograph for Determining Corrected Geomagnetic Local Time, Latitude, and Longitude for High Latitudes in the Northern Hemisphere," AFCRL-70-0422 (1970).